Biomicrofluidics REVIEW scitation.org/journal/bmf

Recent advances in acoustic microfluidics and its exemplary applications

Cite as: Biomicrofluidics **16**, 031502 (2022); doi: 10.1063/5.0089051
Submitted: 22 February 2022 · Accepted: 24 May 2022 ·
Published Online: 13 June 2022

Yue Li,[1] Shuxiang Cai,[1] Honglin Shen,[1] Yibao Chen,[1] Zhixing Ge,[2] and Wenguang Yang[1,a)]

AFFILIATIONS

[1]School of Electromechanical and Automotive Engineering, Yantai University, Yantai 264005, China
[2]State Key Laboratory of Robotics, Shenyang Institute of Automation, Chinese Academy of Sciences, Shenyang 110016, China

[a)]**Author to whom correspondence should be addressed:** yangwenguang@ytu.edu.cn

ABSTRACT

Acoustic-based microfluidics has been widely used in recent years for fundamental research due to its simple device design, biocompatibility, and contactless operation. In this article, the basic theory, typical devices, and technical applications of acoustic microfluidics technology are summarized. First, the theory of acoustic microfluidics is introduced from the classification of acoustic waves, acoustic radiation force, and streaming flow. Then, various applications of acoustic microfluidics including sorting, mixing, atomization, trapping, patterning, and acoustothermal heating are reviewed. Finally, the development trends of acoustic microfluidics in the future were summarized and looked forward to.

I. INTRODUCTION

Microfluidics is a technical method that uses submillimeter size microchannels to manipulate objects or fluids at the micro- or nano-scale. During the past several decades, microfluidics technology has attracted a wide range of interest and research due to its exceptional advantages such as lower sample consumption, convenience of use, and fast reaction.[1–5] The field of microfluidics has completely changed the way of handling and manipulating samples in microsystems. At present, to achieve more precise control and flexible manipulation, optical, electrical, magnetic, acoustic, and hydrodynamic systems were introduced to form microreactors.[6–9]

Among various technologies, microfluidics based on acoustics has been recognized as an efficient method for manipulation at the micro-scale and has been gaining popularity in recent years due to its unique advantages. Acoustic microfluidic devices manipulate particles and cells through acoustic waves. This is a contact-free manipulation that avoids physical contact with the target object and can effectively prevent sample contamination.[10] Compared with magnetoelectrophoresis and dielectrophoresis (DEP), the acoustic field has a weaker influence on the viability and characteristics of the samples under the proper frequency range.[11] In addition, the power intensity and frequency of the majority of acoustic microfluidics resemble those of the devices used in ultrasound imaging, which has been widely used in prenatal diagnostics.[12] Centner *et al.* indicated that the survival rate of red blood cells is high (>80%) under different acoustic pressures, and it is demonstrated in the experiments where the ultrasound was used to induce the delivery of molecules to red blood cells.[13,14]

The purpose of this Review is to provide a systematic summarization of the recent advances in acoustic-based microfluidics (Fig. 1). Particularly, we first discuss the principles of acoustic waves and the mechanism of controlling objects in microfluidics. In addition, we also highlight the unprecedented opportunities of acoustic microfluidics in chemical and biomedical applications combined with the current research status of this technology. Finally, limitations and future research directions of the acoustic microfluidics are also presented.

II. PRINCIPLES AND MECHANISM OF ACOUSTIC MICROFLUIDICS

A. Acoustic wave

Generally, bulk acoustic waves (BAWs) and surface acoustic waves (SAWs) are the two main types of acoustic waves. An elastic wave that propagates along the surface of a medium is called SAW, and its amplitude decays with the depth index

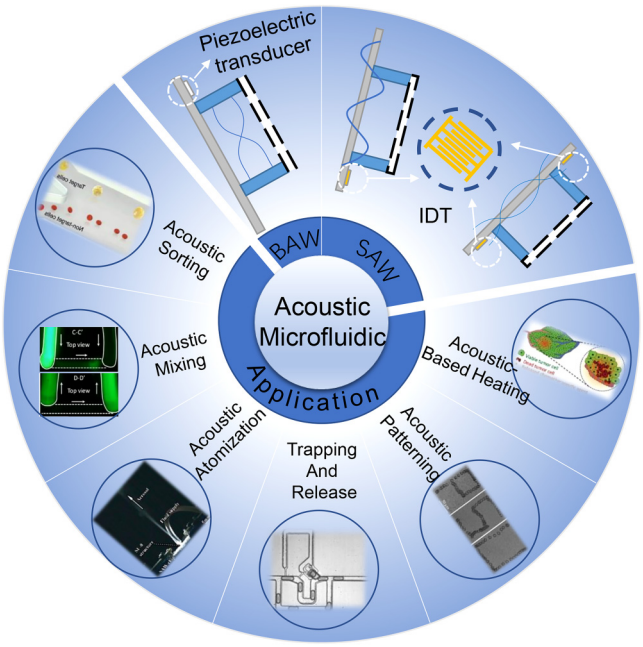

FIG. 1. Development, structures, and applications of acoustofluidics.

of the surface. The principle of SAW was first explored by Lord Rayleigh.[15] In 1965, White and Voltmer invented the interdigitated transducer (IDT).[16] According to the different generation methods, SAWs can be categorized into two types: traveling wave surface acoustic waves (TSAWs) and standing wave surface acoustic waves (SSAWs). TSAWs can be regarded as SAWs that are emitted from an acoustic source and radiated outward in a single direction on a substrate [Fig. 2(a)]. The interference of two SAWs transmitting in the reversed path is the main cause of SSAWS, which can create fixed pressure nodes (PNs) and antinodes (PAs) in a fixed domain [Fig. 2(b)].[17,18] Conversely, BAWs are a type of elastic waves that propagate in a medium as a longitudinal and a transverse wave, which is generally generated by a piezoelectric transducer [Fig. 2(c)]. Table I is a brief summary of the differences and characteristics of SAW-based and BAW-based acoustic microfluidics; microfluidics based on different acoustic waves will also be described in Sec. III.

B. Acoustic radiation force and acoustic streaming

1. Acoustic radiation force

Acoustic waves propagate through the medium with a definite amount of energy and momentum, and the forward average pressure is generated in it whose direction is the same as the direction of sound propagation. The primary radiation force (PRF) and the secondary radiation force (SRF) are the two types of acoustic radiation force. The formulation of the PRF in the traveling wave was proposed by King in 1934,[19] which is given by

$$F = 2\pi p_l |A|^2 (kR_p)^6 \frac{1+\frac{2}{9}(1-\lambda_\rho)^2}{(2+\lambda_\rho)^2}, \tag{1}$$

$$\lambda_\rho = \frac{\rho_l}{\rho_p}, \tag{2}$$

where A is the amplitude of the velocity potential, R_p is the radius of the particle, λ is the wavelength, ρ_p is the density of the particle, and ρ_l is the density of the fluid; k is the wavenumber of the acoustic radiation, which is defined by $2\pi/\lambda$.

The PRF generated by a standing wave is composed of an axial component and a transverse component. According to the density, size, and acoustic contrast factor of the particle and fluid, particles are pushed into the node or antinode of the acoustic field, and this process is predominated by the axial acoustic radiation force,[19,20]

$$F_a = -\left(\frac{\pi p_0^2 V_p \beta_l}{2\lambda}\right)\Phi(\beta,\rho)\sin(2kx), \tag{3}$$

$$\Phi(\beta,\rho) = \frac{5\rho_p - 2\rho_l}{2\rho_p + \rho_l} - \frac{\beta_p}{\beta_l}, \tag{4}$$

where Φ is the acoustic contrast factor; the density and compressibility of the particles and the medium determine Φ. ρ_0 is the acoustic pressure amplitude, x is the distance from the acoustic pressure node, V_p is the volume of the particle, and β_p and β_l characterize the compressibility of the particle and the surrounding fluid.

When the particles approach the node position under the action of the axial component of the PRF, the effect of the transverse component of the PRF can no longer be neglected,[21]

$$F_t = 3d_p^3 \frac{\rho_p - \rho_l}{2\rho_p + \rho_l} \nabla\langle E_{ac}\rangle, \tag{5}$$

where $\nabla\langle E_{ac}\rangle$ is the acoustic energy gradient.

Suspended particles in the standing wave field also experience an SRF induced by scattering waves from other particles. However, SRF is meaningful only if the distance between the particles is short. This interparticle force is also called Bjerknes force.[22] The radius of the particle, the central distance between the particles, and the expression of SRF on particles in an infinite medium are given by[23]

$$F_{SRF} = 4\pi a^6 \left[\frac{(\rho_p - \rho_l)^2(3\cos^2\theta - 1)}{6\rho_l d^4} v^2(x) - \frac{\omega^2 \rho(\beta_p - \beta_l)^2}{9d^2} p^2(x)\right], \tag{6}$$

where a is the particle radius, d is the central distance of the particle, and θ is the angle between the connection lines of the particle and the direction of the acoustic wave. If the force calculated is less

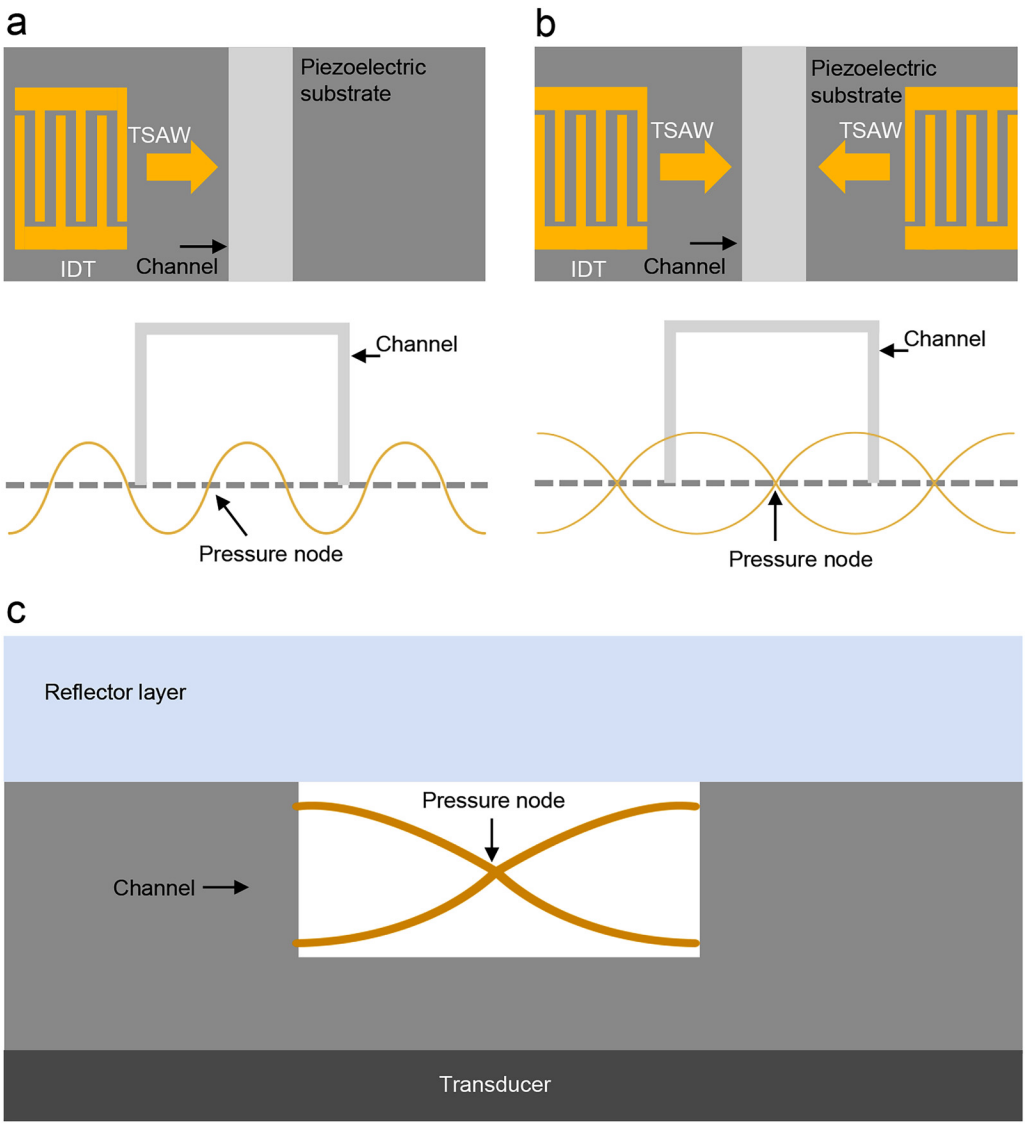

FIG. 2. Schematic diagram of different types of acoustic waves propagating in a microchannel. (a) Traveling surface acoustic waves (TSAWs). (b) Standing surface acoustic waves (SSAWs). (c) Bulk acoustic waves (BAWs).

than zero, it proves that the force between the particles is attraction, whereas a positive value represents a repulsive force between the particles. The first term in brackets is the velocity component, which depends on $v(x)$, and the second term in brackets is the pressure component, which depends on $p(x)$.

Bubbles are a common tool in acoustic microfluidics, and the SRF related to bubbles has been extensively studied, including the interaction between bubbles, the interaction between a bubble and a particle, and the interaction between a bubble and a droplet.[24,25] The equation for the SRF between a bubble and a particle is given by

$$F_p = 4\pi\rho_l \frac{\rho_l - \rho_p}{2\rho_p + \rho_l} \frac{R_b^4 R_p^3}{d^5} \omega^2 \xi^2, \tag{7}$$

where R_b and R_p are the radii of the bubble and the radius of the particle, respectively. d represents the distance between the bubble and the particle, ω is the frequency of the bubble oscillation, and ξ represents the amplitude of the bubble oscillation.

TABLE I. Acoustic microfluidics based on different acoustic waves.

		SAW-based device	
	BAW-based device	TSAW	SSAW
Source of generation	A piezoelectric transducer	One interdigitated transducer	Two interdigitated transducers
Propagation method	Vertical propagation in the body of the material	Propagates along the surface of the substrate and leaks into the liquid	
Substrate material	High characteristic acoustic impedance	Characteristic acoustic impedance similar to fluid	
Operating frequency	500 KHz–5 MHz	10 MHz–1 GHz	
Advantages	High throughput; ability to handle large sample volumes	Miniaturization; less energy consumption; ability to hand smaller sized micro-objects	

The SFRs of large diameter particles (particle diameter close to half of the wavelength) were investigated by Habibi *et al.*[26] The results indicate that the resonant frequency of the solid sphere has a significant effect on SRF. In 2018, by investigating the SRF between three different sizes of polystyrene particles, Mohapatra *et al.* found that SRF decreases with decreasing particle size and increases with decreasing particles' center distance.[27] By investigating the SRF between cells and particles in microchannels, Saeidi *et al.* found that under some conditions, the SRF acting on biological cells can dominate over the PRF.[28] When RBCs move toward the pressure node under the PRF, they are captured by silica particles located at a short distance from the pressure node between the node and the antinode. This explores the prospect of the application of secondary acoustic forces in the separation, trapping, and sorting of cells.

Suppose that the wavelength of the acoustic wave is much larger than the radius of the suspended particles, the mechanism of particle movement in the standing acoustic field can be briefly described as follows.[29,30] First, the particles migrate in the direction of the acoustic wave toward the pressure node, and the process is dominated by the axial component of the acoustic radiation force. When the particles are located at the plane of the pressure node, the transverse component of the acoustic radiation force becomes dominant, and the particles approach each other under its action. Then, due to the force scattered from nearby particles, the particles will further migrate toward the central axis of the standing wave field. The particles are, therefore, densely packed together at the pressure node. Thus, the particles are closely packed together at the position of pressure nodes.

2. Acoustic streaming

Acoustic streaming and microstreaming are two main types of streaming flow. When the acoustic energy in the fluid is attenuated, the high-amplitude acoustic oscillations generate a gradient, resulting in acoustic streaming. Microstreaming is caused by the vibration of micro-objects in the fluid.[31] The Stokes drag force is caused by both types of flows. The Stokes drag force applied on the particles at low Reynolds number can be expressed by the following formula:[32]

$$F_D = -6\pi\mu R_p v, \tag{8}$$

where μ represents the fluid viscosity, v is the relative speed between the fluid and the particle, and R_p represents the particle radius.

There are two forces in the acoustic standing wave field that influence particles inside the microchannel: one is the acoustic radiation force and the other is the Stokes drag force due to acoustic streaming. As the PRF is proportional to the volume of the particle, for smaller particles ($<1\,\mu$m), the drag force is caused by acoustic streaming over the PRF.[33] Acoustic streaming is beneficial for acoustic mixing. However, the fluid velocity associated with acoustic streaming is small compared to the fluid velocity on the channel, so that the effect of the drag force caused by acoustic streaming is usually difficult to work.

III. TYPICAL ACOUSTIC MICROFLUIDIC DEVICES

Acoustic microfluidic chips can be made from a variety of materials. Silicon has been extensively used as an early material for microfluidics.[34,35] Polydimethylsiloxane (PDMS), glass, polycarbonate, and polymethyl methacrylate are the main materials for microfluidic device fabrication. The choice of resonator material depends on the type of resonating system used for manipulation.[33] The construction of different typical acoustic microfluidic devices is briefly described in this article.

A. SAW-based acoustic microfluidic

The surface waves are generated by interdigitated electrode transducers (IDTs). These IDTs are located outside of the microchannel and typically manufactured in PDMS with the technology of soft lithography. The IDT consists of multiple metal electrodes and is manufactured by metal evaporation and liftoff to form metal strips on a piezoelectric substrate (generally $LiNbO_3$). Typically, microchannels are manufactured by molding PDMS on silicon or SU-8 master.[36,37]

The structure of an IDT is closely related to the characteristics of the generated SAW, and the parameters of its structure are composed of the number of pairs of fingers, the aperture, and the length of the period of metallic fingers. Therefore, SAW with different characteristics can be generated by changing the structure of the IDTs. Designing IDTs of different wavelengths can obtain SAW devices of different frequencies, for example, a slanted finger IDT [Fig. 3(a)], a focused IDT [Fig. 3(b)], and a chirped IDT [Fig. 3(c)].

A slanted finger IDT can be regarded as a string of thin IDTs with evenly spaced fingers, and the narrow SAWs can be generated

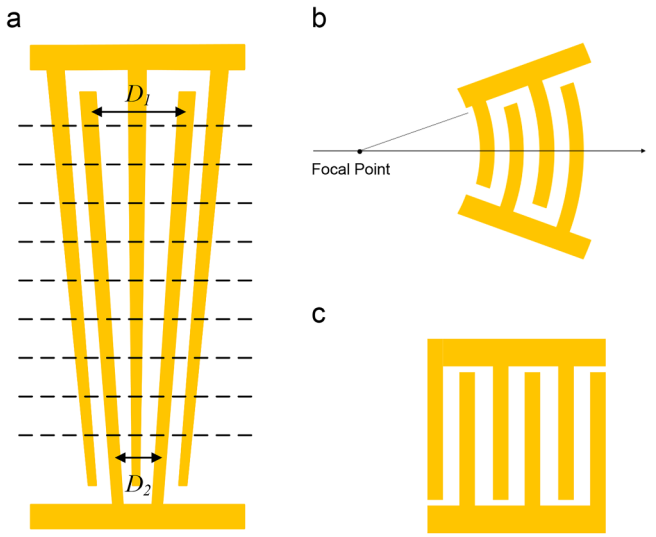

FIG. 3. The configuration diagram of IDT with different structures. (a) A slanted IDT; (b) a focused IDT; (c) a chirped IDT.

by it.[38] The period of the metal finger for each channel can be obtained from the following equation:

$$D_i = \lambda = \frac{c}{f_i}, \tag{9}$$

where λ represents the wavelength of the SAW, c represents the velocity of the SAW, and f_i represents the resonance frequency of the sub-channel.

The electrodes of the focusing IDT are curved. The energy of the SAW can be focused on and concentrated into a focal point by these concentric electrodes.[39]

A chirped IDT has a linear gradient within the circumference of their fingers, which gives it a broader range of resonate frequency.[40] The distance between the electrodes is given by

$$\lambda_{SAW} = \frac{v_{SAW}}{f}. \tag{10}$$

B. BAW-based acoustic microfluidic

Piezoelectric transducers are generally located under the microchannels, generating BAW that is perpendicular to the direction of excitation incidence, and the frequency is adjustable ($f = \omega/2\pi$). On the other hand, the generation of BAW relies on reflection between microchannels made of materials.[33,41]

The platform of BAW acoustophoretic for droplet handling operation is shown in Fig. 4.[42] The microfluidic channels with a height of 200 μm are located on a silicon substrate, and the front surface of the chip is covered with a glass wafer with a thickness of 500 μm. The piezoelectric transducer is glued underneath the microchannel, and by applying an electrical signal, the piezoelectric transducer generates an acoustic field in the fluid of the microchannel.

IV. EXEMPLARY APPLICATIONS OF ACOUSTIC MICROFLUIDICS

A. Acoustic sorting

The successful sorting of needed substances from the solutions is a key step in a variety of applications and has profound

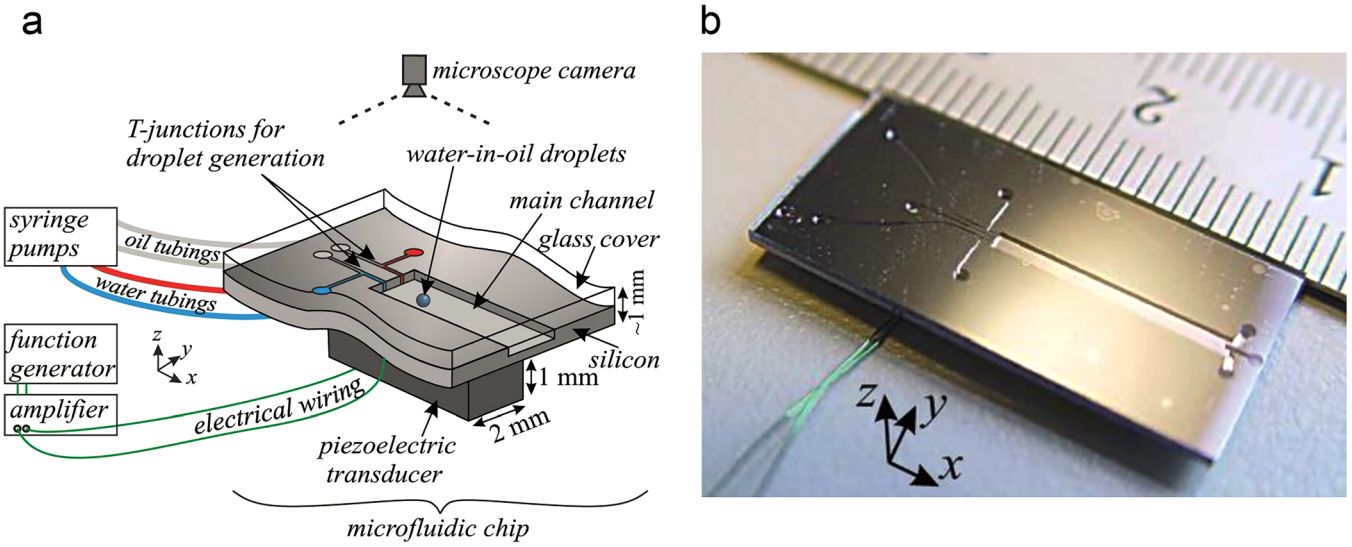

FIG. 4. (a) Schematic diagram of a BAW-based microfluidic device for droplet manipulation. (b) Photograph of the device front side. From Leibacher *et al.*, Lab Chip **15** (13), 2896–2905 (2015). Copyright 2015 Author(s), licensed under a Creative Commons Attribution (CC BY) License.[42]

significance in biological research and clinical studies.[43,44] Most traditional sorting methods have drawbacks, such as complex pre-work, heavy instruments, and large amounts of samples, that make them contrary to current development trends. Therefore, acoustic microfluidic sorting has emerged as an alternative method with huge potential that meets the requirements of new developments. Due to the advantages in sorting speed and throughput, fluorescence-activated cell sorting (FACS) is one of the commonly used single cell sorting methods. FACS is a technology in which the cells to be tested are dyed with fluorescent dyes, encapsulated in droplets, activated by a laser to generate fluorescence, and an electric field is exerted to laterally move the cells that need to be sorted.[45,46] However, this technology is subject to some limitations, such as the large volume of samples required and the complexity of the operation. In addition, samples are prone to cross-contamination and the system is prone to blockage. Compared with traditional methods, acoustic-based cell sorting is a gentler treatment method.

Combining the traditional FACS and fluorescence-activated droplet sorting with acoustic sorting, Schmid *et al.* proposed a multifunctional microfluidic fluorescence-activated cell sorter with the ability to sort cells or droplets at an ultrahigh rate (several kilohertz) and was independent of their size and contrast of the target objects, which has important implications for the sorting of bacteria and viruses.[47] According to the intensity of the fluorescence signal, the cells and droplets were driven and deflected by the SAW generated by the IDT, so as to realize the sorting of the target objects. Inlet channel A was responsible for delivering the sample, channels C located at the bottom led to the sheath flow, channel B located at the top was used to dilute the sample concentration to prevent sample aggregation, and the sample was concentrated in the middle of the microchannel by the action of channels B and C together. If the fluorescence intensity of the sample did not reach the threshold, the sample was delivered along the flow trajectory to the waste outlet I. Otherwise, the SAW activated by the IDT E coupled into the fluid along with the narrow path F, and the drag force caused by acoustic streaming deflected and guided the sample to the collection outlet H. Ding *et al.* introduced a multichannel cell sorting device based on SSAW, which consisted of a PDMS channel and a pair of chirped IDTs.[48] By using different frequencies of acoustic waves to vary the position of the pressure node of SSAW, the human white blood cell HL60 was accurately guided to several different microchannel outlets. Compared with other methods for cell sorting, this method enabled the sorting of cells to multiple outlets, realized the parallelization of cells sorting, and improved the accuracy of cell sorting.

In order to further improve the sorting rate of microfluidics for cells, a TSAW-based cell sorting device was proposed by Ung *et al.*[49] As shown in Fig. 5(a), the IDT was positioned next to the microchannel of the microfluidic device. The sample and the sheath flow into the sorter through different functional inlets, and the flow-focusing nozzle feeds the sample into the sorting area marked in red. When a target cell was detected, acoustic waves sort the cells, deflect them away from the sorting area, and send them to the sorting outlet. The slanted groove was located above the sorting area and was used to enhance the acoustic deflection of the cells. Because of vertical constriction, the sheath flow confined the cell sample laterally downward to the bottom of the microchannel, and the flow of the fluid at the base is largely undisturbed. When an acoustic wave acted on the target cells, the cells were acoustically deflected into the groove and were guided by the groove to create a flow, which allowed the cells to pass through the sorting area laterally. The device has a high sorting rate that approached the one of the FACS device and achieved a sorting purity of 92% when working at a speed of 1000 events/s. The maximum sorting rate could be up to 9000 events/s while the purity is 60%.

In blood, compared to the size of white and red blood cells, while platelets and bacteria are smaller in size;[50] the separation of red and white blood cells is important for the diagnosis of diseases.

Acoustic radiation force generated by SSAW was employed by Shamloo and Boodaghi to achieve acoustic sorting of platelets, red blood cells, and white blood cells in different sizes.[51] The magnitude of the force increases as the diameter of the particle increases. The simulation of the cell trajectories at different pressures is shown in Fig. 5(b). Different sizes of particles are employed for the simulation. The trajectory of a particle without acoustic radiation force is shown in Fig. 5(b)(i); this happened because the drag force exerted on the particles prevented the particles from moving in the direction of the particle path. As shown in Fig. 5(b)(ii), when $\Delta V = 1$ V, the acoustic radiation force was too small to affect the movement of particles of three sizes, so that all sizes of cells flow out of the side outlet. For $2 < \Delta V < 4$ V, red blood cells and platelets of relatively small size flow out of the side outlet, and white blood cells flow out of the intermediate outlet, thereby realizing the separation of white blood cells [Fig. 5(b)(iii)]. When $4\text{ V} < \Delta V < 6$ V, the smallest size platelets were sorted [Fig. 5(b)(ii)].

The detection of circulating tumor cells (CTCs) is critical in the diagnosis and prognostic assessment of tumors.[52,53] To improve the sorting performance, Wang *et al.* made an acoustic microfluidic device with multi-stage SAWs, which consisted of a pair of straight IDTs and focused IDTs.[54]

The focusing of the sample was achieved by straight IDTs, which generated SSAWs that focused CTCs and red blood cells onto the pressure nodes in the acoustic field. The TSAWs were generated by the focused interdigital transducers (FIDTs); according to the difference in the size of CTCs and red blood cells, the CTCs and red blood cells were separated by the acoustic radiation force. The unidirectional radiation force generated by TSAW increases the sorting capacity of the device. According to this mechanism, it was proved that when the TSAW period was 720 k, about 90% of U87 could be separated from the red bold cells [Fig. 5(c)]. Zhou *et al.* combined inertial focusing and acoustic separation to enrich the breast cancer cells diluted in whole blood sample at least 2500 times and to maintain cell viability of $91\% \pm 1\%$.[55] The schematic of the combination of inertial sorting based on the size and the fluorescence-activated sorting based on acoustics is shown in Fig. 5(d). A reverse wavy channel was the modified microchannel structure that enabled the enrichment of cancer based on the size. When the target cells with a fluorescent label were detected, an electrical signal was applied to FIDTs, so that a highly focused acoustic beam was generated by the FIDT, and thereby acoustic streaming was used to sort the target cells. The device adopts a novel channel design that enabled high-throughput pre-enrichment

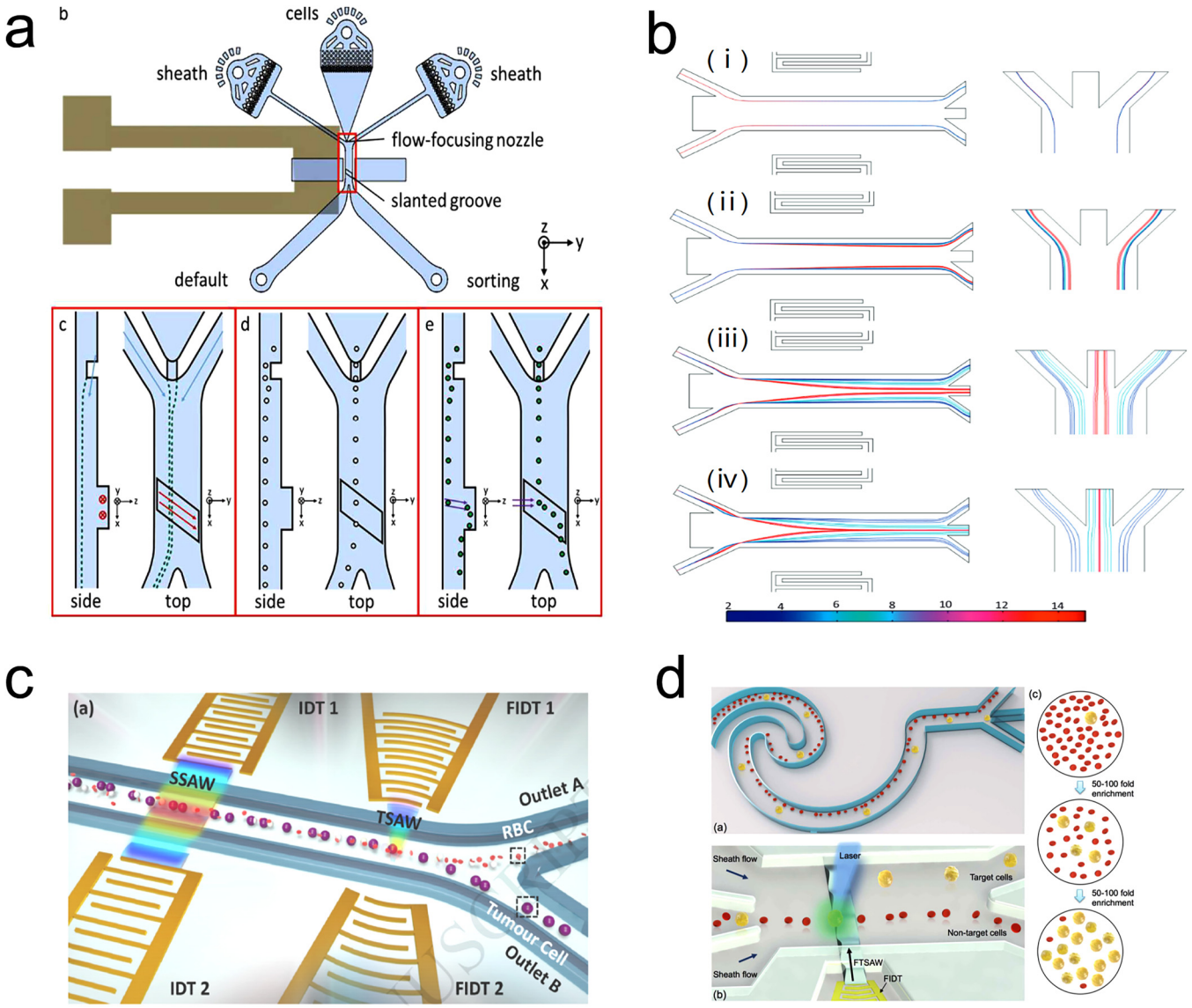

FIG. 5. (a) A design using inclined grooves to enhance surface acoustic wave sorting and a schematic diagram of its sorting process. From Ung *et al.*, Lab Chip **17**(23), 4059–4069 (2017). Copyright 2017 Author(s), licensed under a Creative Commons Attribution (CC BY) License.[49] (b) Numerical simulation of cell trajectories: (i) Acoustic radiation force is absent, (ii) $\Delta V = 1$ V, (iii) $\Delta V = 3$ V, and (iv) $\Delta V = 5$ V. The color legend shows the diameter of the particles in μm. Reproduced with permission from Shamloo and Boodaghi, Ultrasonics **84**, 234–243 (2018). Copyright 2018 Elsevier B.V.[51] (c) Schematic illustration of the multi-stage device and tumor cell isolation. Reproduced with permission from Wang *et al.*, Sens. Actuators B **258**, 1174–1183 (2018). Copyright 2018 Elsevier B.V.[54] (d) Schematic diagram of the hybrid acoustic sorting device for cell separation. From Zhou *et al.*, RSC Adv. **9**(53), 31186–31195 (2019). Copyright 2019 Author(s), licensed under a Creative Commons Attribution (CC BY) License.[55]

prior to separation, providing a promising method for the sorting of rare cells in cancer diagnosis and treatment.

The advantage of BAW-based acoustic microfluidics is that the piezoelectric transducer is integrated externally. However, the rate of BAW-based acoustic separation is not as excellent as that of SAW and is prone to problems at high throughput.[56] Devendran *et al.* presented a method for separating particles in trace amounts of sample by size and achieved the sorting of polystyrene particles with diameters of 3 and 10 μm.[57] Leibacher *et al.* proposed a BAW-based acoustic microfluidic for droplet handing that included the sorting of droplets.[42] Different wavelength modes were generated by changing the acoustic frequency, thereby sorting out droplets of different sizes.

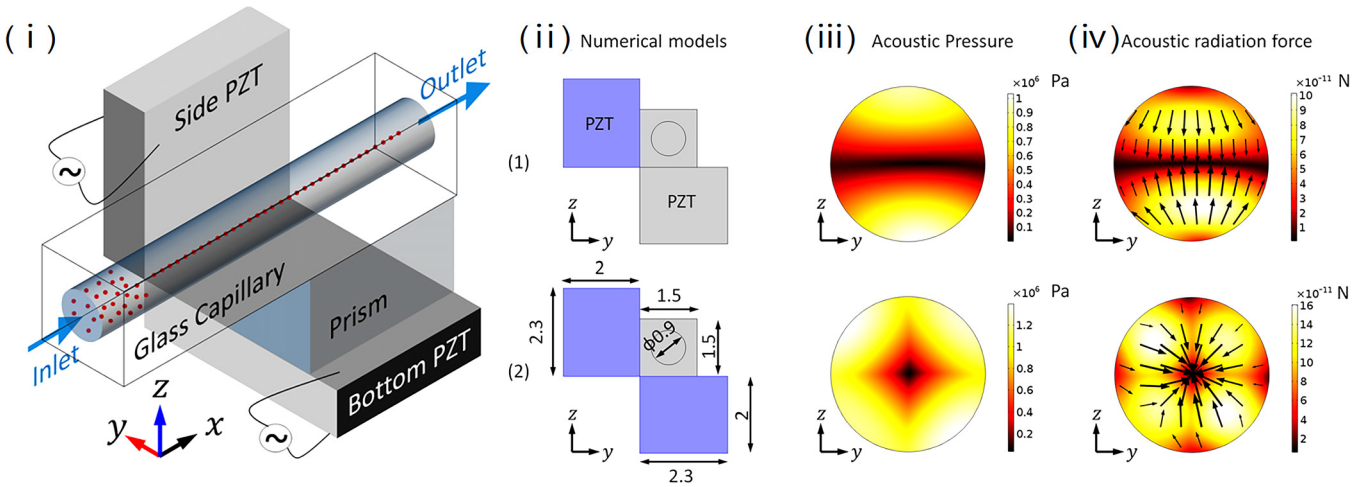

FIG. 6. Schematic presentation of 2D focusing of microparticles and the mechanisms of focusing two-dimensional particles in glass capillaries under different ultrasonic excitations. Reproduced with permission from Lei *et al.* Appl. Phys. Lett. **116**(3), 033104 (2020). Copyright 2020 AIP Publishing LLC.[58]

Compared with SAW-based microfluidics, BAW-based microfluidics allows various configurations of geometries, for example, the placement position of the ultrasonic transducer is more flexible.

Lei *et al.* designed a bulk acoustic microfluidic device, which mainly consisted of two orthogonally placed PZTs, a glass capillary with square outside and round inside [Fig. 6(i)].[58] The ability to sort the particles was demonstrated by focusing on the polystyrene particles of 10 μm in the solution into the center of the microchannel. There are two cases of particle sorting: (1) excitation of the bottom transducer and (2) excitation of both transducers [Fig. 6(ii)]. The acoustic pressure field models for these two cases are presented in Fig. 6(iii). When both transducers were activated at the same time, the position of the pressure node was located in the center of the microchannel, and the primary acoustic radiation force acted on the particle to drive it from the antinode to the pressure node [Fig. 6(iv)].

Similar to SAW-based microfluidics, bacteria can also be treated with BAW-based acoustic microfluidics. A BAW-based polystyrene microfluidic device was produced by Dow *et al.*[59] The device was applied to pretreat blood samples to facilitate the detection of bacteria by a bacteriophage-based luminescence analysis.[60] The results demonstrated that compared to the unpurified blood sample, the device provided a method with substantially higher detection limits. Blood samples were treated with this acoustic sorter to remove more than 85% of the red blood cells and the output of bacteria reached more than 40%.

The main microfluidic active sorting technologies are FACS, magnetic sorting, optical sorting, dielectrophoresis, and acoustic sorting. FACS is the mainstream cell sorting method due to its excellent sensitivity of fluorescence detection.[61,62] However, this technology requires expensive and heavy equipment, which could lead to channel blockage and sample pollution in the sorting process. To reduce costs and achieve device portability, other sorting techniques have been proposed, but each has different limitations. Magnetic sorting has low sensitivity, the process of labeling cells with magnetic beads is time-consuming, dielectrophoretic sorting is largely reliant on the size of the object, and optical sorting has low throughput.[17,63,64] Acoustic sorting can be divided into two types according to acoustic modes, SAW-based sorting and BAW-based sorting, which mainly rely on acoustic radiation force for manipulation. Compared with other sorting technologies, it has the advantages such as non-contact, label-free, and high efficiency, and the throughput can reach the same level as commercial FACS. It can realize the sorting of cancer cells, red blood cells, white blood cells, bacteria, and viruses and has great potential in the field of biomedicine and chemical analysis.

B. Acoustic mixing

Mixing is a key process in many chemical analysis and synthesis processes.[65] It is important for a range of applications, including biomedical research and medical analysis, and it enables the research of complex reactions and the synthesis of new materials and nanoparticles.[66–68] Microfluidics has become a reliable mixing tool due to its high throughput and few sample requirements. However, because of the small size of microchannels and low Reynolds number, mixing requires a longer time. Various techniques have been developed to improve the mixing efficiency, and acoustic microfluidic chips have been extensively used due to their biocompatibility and simplicity of fabrication.

To reduce the electrical power consumption of acoustic mixing, Ahmed *et al.* proposed a simple fabricated and efficient mixing micromixer, which consisted of a microchannel made of single-layered polydimethylsiloxane and an IDT under the microchannel. The SAW applied acoustic streaming flow (ASF) to the sample inside the microchannel to achieve fluid mixing.[69] Coupling between the SAW and the fluid is adapted to produce ASF, which disturbs the laminar flow in the absence of ASF, leading to mixing inside the

microchannel. Compared with other SAW-based micromixers, this device can work at higher throughput and lower power consumption through direct coupling between the SAW and the fluid. With an applied voltage of 12 V, the mixing efficiency of the device is more than 90%, and the capacity of throughput could reach 200 μl/min. Nam *et al.* made the microfluidics filled with a conductive liquid (CL) in order to replace the patterned solid metal electrodes.[70] For the first time, CL-based electrodes were applied to generate strongly focused surface acoustic waves (FSAWs) in a microchannel and the concentrated acoustic force generated by FSAW.

De-ionized (DI) water and fluorescent particle suspensions in the microchannel were rapidly mixed under a driving voltage of 21 V; the throughput reached 120 μl/min, and the mixing efficiency was higher than 90%. The mixing mechanism is shown in Fig. 7(a), and fluids A and B entered the micromixer through two inlets, respectively. The FSAWs were generated by an electrode channel filled with CL. The direction of acoustic streaming caused by the longitudinal pressure wave was vertical to the direction of flow, which led to the mixing of the liquids in the microchannel. Nam and Lim used three-dimensional dual surface acoustic waves (3D-dSAWs) generated by two IDTs to induce internal swirling inside the microchannel in a single direction to achieve mixing.[71] Moreover, when the voltage was 18 V, the yield of the 3D-dSAW mixer was further increased to 120 μl/min, while the efficiency of mixing was up to more than 95%. The working principle of the 3D-dSAW microfluidics is shown in Fig. 7(b), and the illustration at the lower left position of Fig. 7(b) shows the device diagram of the 3D-dSAW mixer. When the RF signal was applied, the highly concentrated acoustic forces were generated by FIDT, which was deposited on piezoelectric substrates. In addition, a unidirectional SAW was generated by superimposing the transmission and reflection of the SAWs. FIDTs located on top and bottom substrates generated two FSAWs and were coupled with the liquid in the microchannel. FIDTs entered the liquid as a leakage wave to generate a longitudinal pressure wave, which caused a swirling vortex along a single direction in the microchannel and caused rapid mixing of the fluid in the microchannel. To further improve the rate and homogeneity of mixing, Rasouli and Tabrizian presented an energy-efficient acoustic platform based on boundary-driven acoustic steaming.[72]

Targets are encapsulated into nanoliter or picoliter volume droplets by a droplet-based system.[73,74] Collins *et al.* proposed a new method of adopting SAW to selectively produce individual droplets in the picoliter-scale size.[75] The SAW-based droplet generation microsystem was made up of a chamber on the top of the SAW device that was composed of FIDTs, and an improved T-junction was combined with the SAW equipment and the focus point of the FIDT was aligned with the orifice position. The disperse phase fluid and continuous phases produced droplets at the T-junction. This SAW-based system integrates droplet generation,

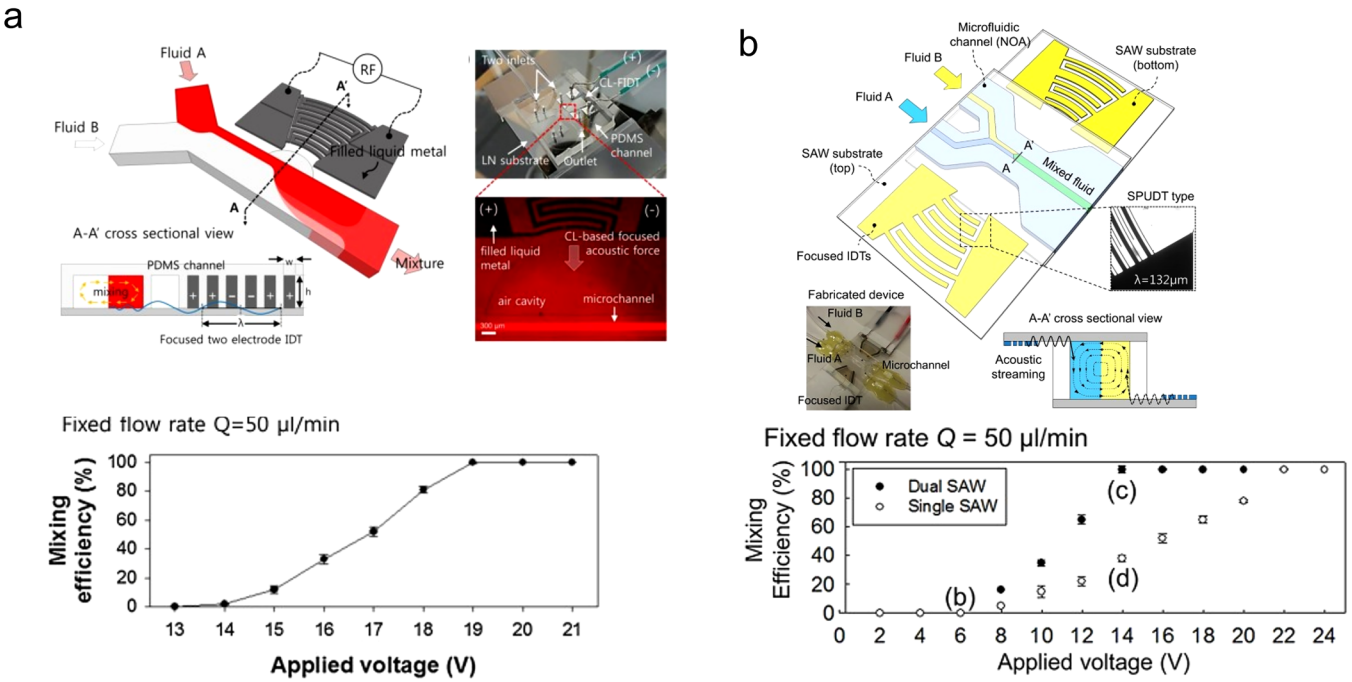

FIG. 7. (a) Schematic of the CL-FSAW-based mixing device. The two fluids are mixed in the microchannel by applying an RF signal to the CL of the FIDT. In the A-A′ cross section view, leaky SAWs influenced the sample in the microchannel. Reproduced with permission from Nam *et al.*, Sens. Actuators B **258**, 991–997 (2018). Copyright 2018 Elsevier B.V.[70] (b) Schematic diagram of the device and the working mechanism of 3D-dSAW microfluidics. Reproduced with permission from Nam and Lim, Sens. Actuators B **255**, 3434–3440 (2018). Copyright 2018 Elsevier B.V.[71]

concentration, and encapsulation in one device, allowing flexible combination with microfluidics.

Nanoparticle has an enormous application range, such as construction of complex materials, cell imaging, nanomedicine, and targeted drug delivery.[76–78] Nanoparticles are usually produced in batches, which require large time scales for mixing the reacting solution and less precise control of mixing times. This results in the development of concentration gradients in the mixing solution, which interferes with the nucleation and impairs the homogeneity and reproductivity of the particles.[79] In order to proceed with high-throughput nanoparticle synthesis, An Le *et al.* designed a star-shaped microfluidic device for mixing.[80] The center of the device was a resonator of controllable thickness with a circular etched hole. This construction was located between the two layers of PDMS. The function of the lower layer was to lead the mixing fluids to the mixing region, and the function of the upper layer was to lead the mixed fluid out. This system could be adapted to a flow rate of 8 ml/min. The micromixer could synthesize nano-diameter budesonide nano-drugs and DNA nanoparticles by mixing DNA solution with polyethylenimine (PEI) at a one to one ratio. The morphology and size of the nanoparticles were strongly related to their employment in different applications. Pourabed *et al.* used acoustic microfluidics to effectively solve the problem of controlling the size of nanoparticles.[81] With this system, a protein–peptide candidate BCA-P114 was synthesized, which consisted of enzyme bovine carbonic anhydrase (BCA) fused with a P114. The size of the BCA-P114 particles was controlled by only manipulating the length and intensity of mixing time under the same physical and chemical status of the protein self-assembly. It was proved that larger particles were formed at 35 ms mixing time, while a shortening of the mixing time to 6 ms produced smaller protein particles.

At low Reynolds numbers, the mixing based on microfluidics relies on the laminar flow, and molecular diffusion is slow. To improve the mixing efficiency, several active mixing methods have been demonstrated, including microstirrers, thermal mixing, electrokinetic mixing, and acoustic mixing.[82–85] Microstirrers use a rotating magnetic field to enhance mixing around the microbar and can achieve precise control of mixing but are not easy to fabricate. Thermal mixing usually requires external heaters, and the application is limited by the fact that heating can inactivate biological cells. Electrokinetic mixing devices are easy to implement and require lower voltage, but they also have obvious disadvantages, such as lack of portability. Acoustic mixers enable fluid mixing by employing acoustic waves to promote the diffusion effect between fluids. The application of acoustic waves in mixing makes the mixing process quick (close to instantaneous mixing), efficient, and homogeneous.

C. Acoustic atomization

SAW-based acoustic atomization is a method for the generation of droplets with size from micrometers to submicrometers, and it has a wide range of applications, such as drug delivery, mass spectrometry, and medical inhalators.[86–89]

To address the limitation of SAW-based fluid atomizers by fluid supply, a SAW-based fluid atomization device was proposed by Winkler *et al.* This device adopted the photostructurable epoxy SU-8 as the material for the microchannel and was fabricated by a new one-layer/double-exposure photolithography approach. The device can achieve high degree of accuracy and mass production.[90] Cheung *et al.* proposed a technique for acoustic atomization by utilizing an oscillating extensional flow around micropillars.[91] The device configuration is shown in Fig. 8(a): the width of the microchannel chamber was 1400 μm and there was a series of 200 μm diameter micropillars arranged in the chamber, and a piezoelectric disk was driven by sinusoidal signal to generate acoustic waves that result in vibrating fluid motion around the micropillars. DI water and light mineral oil were used for the dispersed phase and continuous phase, respectively. The advantages of this technique are the low drive frequency and no external pumping equipment, so it can be used to generate small droplets *in situ*.

Submillimeter mist sprays enable a precise target area control in medical applications due to the advantages of high controllability. Yabe *et al.* proposed a SAW-based atomizer that could generate a narrow mist spray in the submillimeter scale with transverse length.[92] The atomizer was composed of a pair of IDTs and a groove located in the middle of the IDTs. Two types of self-converging atomizers, linear and point atomizers, were experimentally demonstrated, obtained by applying different types of IDTs. The function of the groove was blocking the propagation of SAW on the substrate. The two SAWs traveling along different directions were separated by a groove, resulting in two face-to-face propagating acoustic streaming. The horizontal components of the momentum of the mist steaming from both sides of the groove cancel each other, so as to spontaneously converge in the vertical direction.

The lung has become a noteworthy target for therapeutic administration and a local target for the treatment of lung diseases, as drugs can be delivered to the whole body through the lung.[93,94] Nebulizers have advantages in pulmonary drug administration that cannot be matched by traditional inhalers. There are some of the commonly used nebulizers: jet nebulizer; ultrasonic atomizer, and vibrating mesh nebulizer. However, all of them have different disadvantages: the jet nebulizer is bulky and inefficient, the ultrasonic atomizer tends to denature the drug under large cavitation, and the vibrating mesh nebulizer is easy to be blocked in the automatizing process.[95–97]

Cortez-Jugo *et al.* demonstrated an acoustic microfluidic device for medical pulmonary inhalation that enabled the atomization of epidermal growth factor receptor (EGFR) monoclonal antibodies (mAbs) into an aerosol of 1.1 μm in diameter.[98] A comparison between the fluorescence intensity of antibody-treated cells and the fluorescence intensity of untreated cells revealed that the fluorescence intensity of blocked cells was decreased by 70% compared to untreated cells. This demonstrated that the nebulized antibody maintained the ability to bind to the antigen and blocked the phosphorylation of the antigen.

Chronic lung diseases caused by pathogenic bacterial infections have high morbidity and mortality throughout the world. Compounded by the emergence of drug resistance, it brings about a more serious health threat.[99] Therefore, bacteriophages have been a major focus of attention. Bacteriophages are viruses that attack bacteria, and they are one of the most prevalent and widely distributed parasitic viruses. Unlike bacteriostatic antibiotics, bacteriophages cause lysis of host bacteria. Therefore, the possibility of

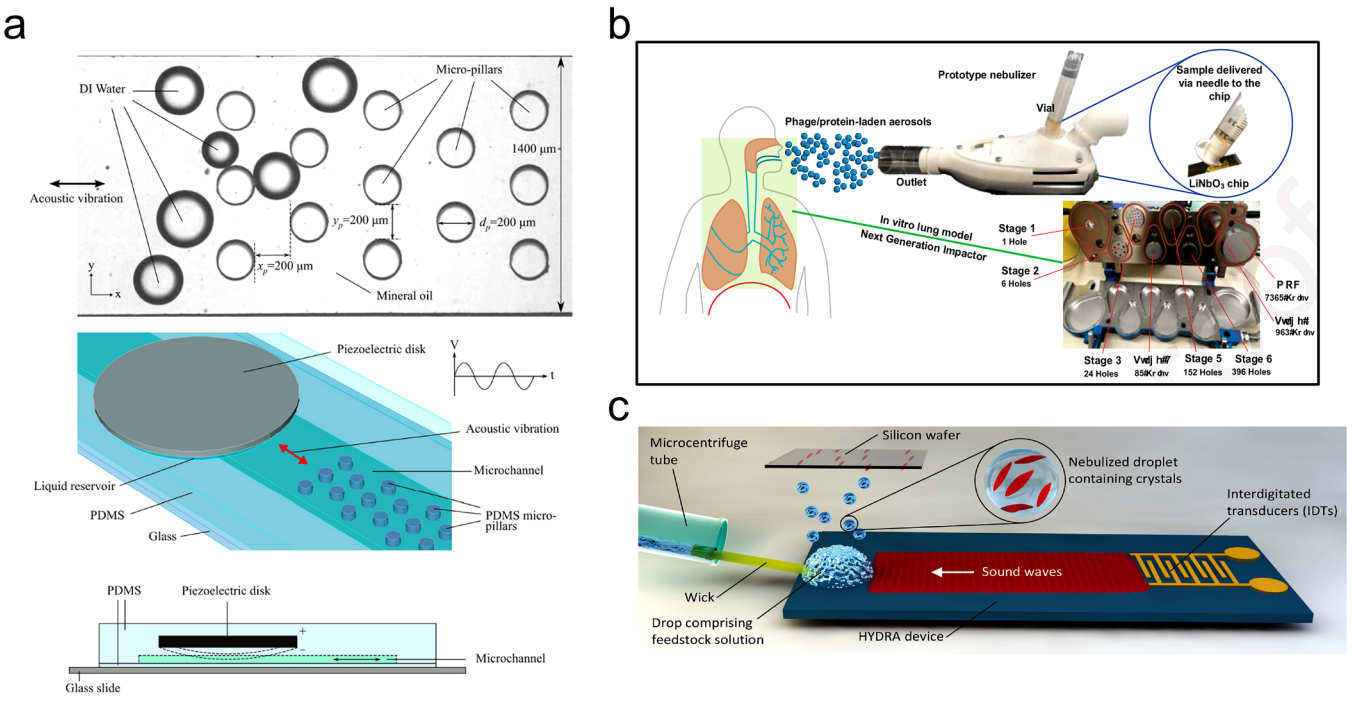

FIG. 8. (a) Schematic diagram of an array of PDMS micropillars and the process of droplet atomization around micropillars. Reproduced with permission from Cheung *et al.*, Appl. Phys. Lett. **105**(14), 144103 (2014). Copyright 2018 AIP Publishing LLC.[91] (b) Schematic of the HYDRA device. Reproduced with permission from Marqus *et al.*, Eur. J. Pharm. Biopharm. **151**, 181–188 (2020). Copyright 2020 Elsevier B.V.[104] (c) Schematic of the acoustomicrofluidic nebulization device and an image of new crystalline morphology produced by the device. Reproduced with permission from Ahmed *et al.*, Adv. Mater. **30**(3), 1602040 (2018). Copyright 2018 John Wiley & Sons.[105]

drug resistance is very small.[100,101] It is also possible to isolate host-specific enzymes from these bacteriophages capable of lysing bacteria, and specific bacteria that are growing or have not yet grown can be killed by lytic enzymes. Thus, the enzymes can be used as therapeutic agents.[102,103] Nebulizers can deliver these different types of medications directly into the lungs. To generate higher output and improve the efficiency and efficacy of nebulization, Marqus *et al.* have combined surface waves with body acoustic waves to nebulize a Myoviridae bacteriophage (phage K) and lytic enzymes (lysozyme), particularly targeting *Staphylococcus aureus*.[104] The device was mounted in the body of the prototype nebulizer as shown in Fig. 8(b), which contained a HYDRA chip consisting of an $LiNbO_3$ substrate and an IDT deposited on the substrate. A feedstock bottle containing 3 ml of phage K or lysostaphin was connected to the upper end of the nebulizer, and the feedstock was delivered to the device via a hypodermic syringe. A HYDRA-based microfluidic atomization device capable of generating new crystal morphologies was proposed by Ahmed *et al.*[105] The evaporation rate directly affects the nucleation pathway of the crystals. The size and size distribution of the crystals are also related to the evaporation rate. This device has a medium evaporation rate, and the diagram of the device is shown in Fig. 8(c). Solution was drawn through the paper core to the edge of the device by the acoustic wave and atomized at the interface between the paper wick and the device, thereby forming micrometer-scale aerosols. Solvent evaporation from the sample causes spontaneous nucleation within the crystalline material.

The reactive substances in the plasma-activated water can deactivate bacteria, but the concentration of the plasma-activated water decreases over time and the storage temperature conditions are harsh, which is not conducive to storage and portability. In order to make plasma-activated water widely used in practice, combining a SAW-based microfluidic nebulizer with a low-temperature atmospheric plasma source, a technique for *in situ* generation of plasma-activated aerosols that can be used for home disinfection was proposed by Wong *et al.*[106] Plasma-activated water was treated with a SAW-based microfluidic atomizer. The plasma-activated water was removed from the reservoir and atomized into an aerosol by a paper tape adhered to the SAW device, and the large surface area per unit volume of liquid within the tape made the treatment time of the liquid shorter.

Nebulizers maintain the activity of the target object when atomizing it and then deliver it. Although the mechanism of nebulizers in detail is not well understood, they have been widely used in biomedical fields. Traditional nebulizers are large, expensive, and poorly portable; in order to address the limitations of traditional nebulizers, many new methods have been proposed. The ultrasonic nebulizer and the vibrating mesh nebulizer mentioned in Sec. IV B are both better alternatives, but both have obvious disadvantages, such as the ultrasonic nebulizer tends to denature the object, and

the meshes of the vibrating mesh nebulizer are prone to clogging. Electrohydrodynamic atomization is also a new method but requires high voltage and has low reliability. Compared with these nebulization technologies, the SAW-based acoustic nebulizer has the advantages of portability, biocompatibility, and precise control and has promising prospects for application.

D. Trapping and release

It is important to capture cell-laden droplets within the microchannel, and they can be used for cell monitoring.

For precise control of droplets in microchannels, Jung *et al.* used focused SAWs for droplet capture; the focused SAWs were generated by slanted finger interdigitated transducer (SF-IDT), the position of the SAW beam was changed with the SAW frequency, and the droplets in the microwell were selectively captured or released by adjusting the position of the beam.[107] The microwells were shaped as bottlenecks such that the droplets to be captured could be confined in the microwell and could overcome the interference of the continuous phase flow and other fluctuations. The capture and release processes are shown in Fig. 9(a). When the SAW beam was aligned with the end of the microwell, the droplet was blocked by the SAW and its velocity rapidly decreased. In the vicinity of the microwell, the acoustic radiation force acted on the droplet so that the droplet can resist the resistance exerted by the continuous phase. After 60 ms, the droplet entered the microwell within 300 ms. The reason that the droplet could be stably trapped by the microwell was that the fluid resistance of the microwell was low and the diameter of the microwell orifice was smaller than that of the droplet. By focusing the acoustic beam to the middle of the microwell, the acoustic radiation force generated by the SAW was applied to the droplet in the microwell, releasing the droplet from the microwell into the main fluid.

With the combination of a tapered interdigital transducer (TIDT) and a multi-height PDMS device, Rambach *et al.* achieved selective passive storage and acoustic release of individual emulsion droplets at high rates of up to 620 drops/s in 20 ms.[108] The PDMS device consisted of five regions that were divided into three different heights. As shown in Fig. 9(b), the green section was the droplet well ($40 \times 50\,\mu m^2$) with a height of 45 μm, which enabled the captured droplets' shape to be undisturbed by the wall; the red section was the restriction of droplet capture; the dark blue section was the inner short bypass channel with a height of 30 μm; and the light blue section was the outer long bypass channel with the same height as the dark blue section. The pressure difference in the well was reduced by bypass channels and the droplets were guided around the well; the SAW generated by the TIDT propagated in the coupling channel (yellow section) for released or captured droplets.

Exosomes are extracellular vesicles with diameter between 30 and 150 mm, containing complex RNAs and proteins, and can be employed as biomarkers for diagnosing diseases.[109] Exosomes are naturally presented in body fluids, and ultra-centrifugation is the commonly used method for exosome extraction. However, this method is tedious and time-consuming and may lead to exosome aggregation and disruption of their integrity.[110] To address the problem of extracting large amounts of exosomes from body fluids, Habibi *et al.* used acoustic wave-activated nano-sieves (SWANS) to capture exosomes and liposomes by employing larger particles (15 μm) in a packed bed.[111] The system consisted of a microchannel and IDTs. The inside of the channel was a row of pillars that created a barrier, and the microparticles in motion were impeded by the barrier; thus, a packed bed was formed. Counter-propagating SAWs were generated by a pair of IDTs coupled into the fluid of the channel and vibrated the microbeads, which exerted a trapping force on the nanoparticles in the resonant mode.

Hydrodynamic trapping is the common method to achieve target micro-object trapping in microfluidic systems.[113] This method is achieved by creating side channels with sufficiently small dimensions. It can be performed by simple and inexpensive devices that do not require additional peripheral equipment, but the

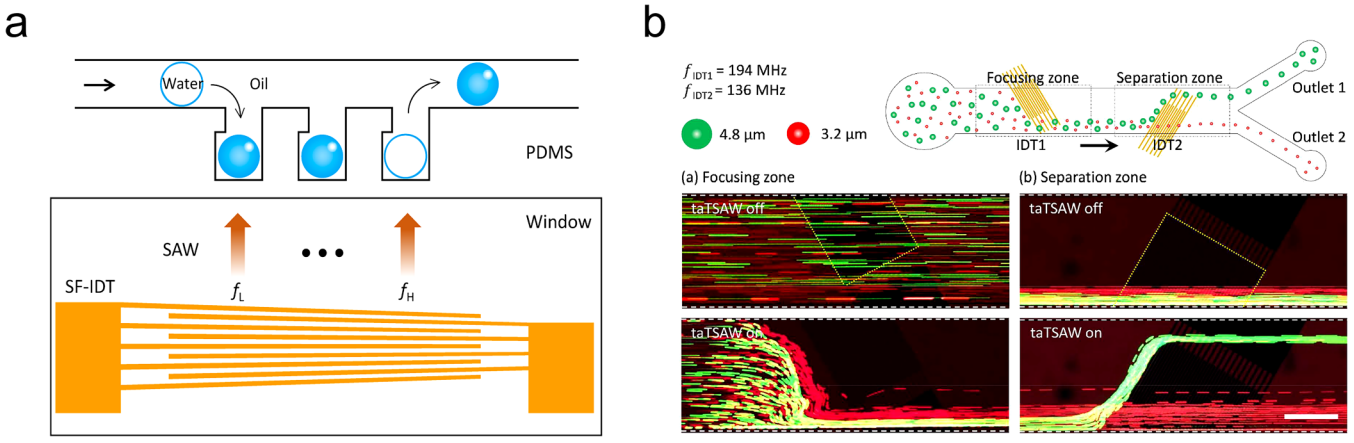

FIG. 9. (a) Illustration of droplet capture and release using acoustic microfluidics. Reproduced with permission from Jung *et al.*, Anal. Chem. **89**(4), 2211–2215 (2017). Copyright 2017 American Chemical Society.[107] (b) SAW-based droplet trapping and release multi-height device. Reproduced with permission from Ahmed *et al.*, Anal. Chem. **90**(14), 8546–8552 (2018). Copyright 2018 American Chemical Society.[112]

accuracy of trapping is low. Optical trapping captures particles and cells by a focused laser beam with high accuracy, but this technique is limited by the laser power. Dielectrophoretic trapping relies on the permittivity and conductivity of the captured object and the liquid medium, and the trapping process could lead to Joule heating. Magnetic trapping depends on permittivity and conductivity in the magnetism of particles and has limitations in its application. Acoustic microfluidics can capture cells or particles without contact. It has the ability to selectively capture target objects in the microchannel by applying acoustic radiation force, which can be precisely performed by adjusting the position of acoustic wave generation. Acoustic-based trapping and release have been widely used in chemical and biological analyses, in particular, for detection and analysis of a cell, with the advantages of non-contact, high throughput, and great precision, and the acoustic energy used is not harmful to cells and does not affect the analysis results.

E. Acoustic patterning

The precise control of positions of cells in three-dimensional microenvironments is a priority during the creation of biomimetic tissue structures that can reproduce natural tissues.[114,115] There have been various methods to realize precise cell micropatterning, and the application of the acoustic wave is a non-intrusive, easy, and low-cost method that provides a new toll for rapid and precise patterning of particles and cells. The experiment of the two-dimensional pattern of particles inside the microchannel driven by SSAWs was proposed by Zheng *et al.*[116] The interactions between acoustic radiated force (ARF) and chain force between polarized particles were investigated. The two-dimensional pattern formed by the particles under the action of two forces is shown in Fig. 10(a). The voltage of 1.5 V was applied to the SSAW device, particles driven by ARF formed a line along the pressure node line (2s), and the ARF was zero at the node. At this time, the chain force dominated the particles to form a two-dimensional array of points at the node region (6s,8s). This research contributed to a deeper comprehension of the trajectory of particles in microchannels under acoustic waves and provided new ideas for precise control of particle pattern formation.

Bouyer *et al.* proposed a bio-acoustic levitation (BAL) technology, and a bulky acoustic radiation force was applied to mammalian cells, resulting in the formation of multilayers in a fibrin three-dimensional environment.[117] With the BAL method, 3D constructs similar in structure to the cerebral cortex were constructed using human stem cell-derived neuro-progenitor cells (NPCs). This demonstrated the utility of the method in bioengineering multilayer 3D tissue substitutes. The BAL assembly device is shown in Fig. 10(b), consisting of a ceramic transducer, a resonance chamber, and a plexiglass reflector. Due to the acoustic radiation force by PZT, the cells moved in a parallel horizontal plane. The distance between the layers of the pattern was proportional to the frequency, and the layer spacing was corresponding to half of the wavelength of the acoustic wave. Therefore, the number of interlayer and the distance between them were dependent on the acoustic frequency.

Naseer *et al.* proposed a new approach to rapidly arrange cells in gelatin methacryloyl (GelMA) by SAWs.[118] This acoustic force-based approach preserved the activity and usability of the cells while controlling their spatial distribution within the 3D construct. The SSAW-based direct patterning of cells was examined by altering the acoustic frequency, the concentration of GelMA, and the length of UV light.

To further investigate the application of SSAW-based contactless patterning techniques in the field of cellular localization under hydrogel environment, an SSAW-based approach was proposed by Nguyen *et al.* to locate microparticles in a microchamber.[119] Due to the different number of IDTs used, the particles could be patterned into 3D spatial lines or lattice-like matrix patterns by the acoustic radiation force generated by SSAW. As shown in Fig. 10(c), when two orthogonal IDTs were activated simultaneously, 3D space lines were formed by the aggregate of microparticles at the nodes. When two pairs of IDTs were activated, a 3D structure similar to a crystal lattice was formed by the particles. The balance of the forces exerted on the microparticle precisely positions the microparticle in the specified position. Depending on the SSAW frequency, particles were realized to be repositioned by moving up and down.

Tao *et al.* explored the effect of the frequency of SAW and structural parameters of microchannels on particle patterning.[120] Figure 10(d)(i) shows the microparticles' alignment at three frequencies and the width of the microparticle traces decreased with the increase in frequency. The position of the particle in the direction of SAW propagation changed according to the phase angle of the SAW. The changes in the position of the two sizes of particles (6 and 10 μm) at different phase angles are shown in Figs. 10(d)(iv)–10(d)(vi). According to Fig. 10(d)(vi), the large size particles moved faster than the small size particles at the same time for the same angle of phase change. The acoustic radiation force drove and captured the microparticle to the node. Once the particle was captured, the microparticle could be moved by adjusting the frequency and phase angle of SAW. Substrates for SAW devices were mostly bulk piezoelectric materials, which were expensive, fragile, and difficult to be integrated with other electrical devices. To overcome these shortcomings, the use of thin-film ZnO/Si as a piezoelectric material achieved particle/cell patterning and 3D operation of yeast cells.

It is well known that microfluidics has the ability to precisely control cells. Finite acoustic pressure nodes are created by acoustic waves within the microchannel. The particles in the microchannel can be arranged in an orderly manner to achieve precise particle manipulation, which is acoustic patterning. The biocompatibility of acoustic waves enables acoustic microfluidic to address many biological challenges, such as tissue engineering. The speed of acoustic patterning is faster compared to other methods.

It is well known that microfluidics has the ability to precisely control cells. Microfluidic cell patterning techniques are available in both contact and non-contact types. Hydrodynamic patterning is a common contact method that achieves cell patterning by confining individual cells to a specific microchannel structure, which is simple to operate but has severe cell loss.[83,121] Non-contact methods include optics, dielectrophoresis, magnetism, and acoustics, which solve the defects of cell damage caused by contact technology. Optical patterning may cause photodamage to biological cells and is unable to accomplish complex patterning. Most DEP-based manipulation of cells requires low conductivity solutions, which limits the application of DEP for cell patterning.

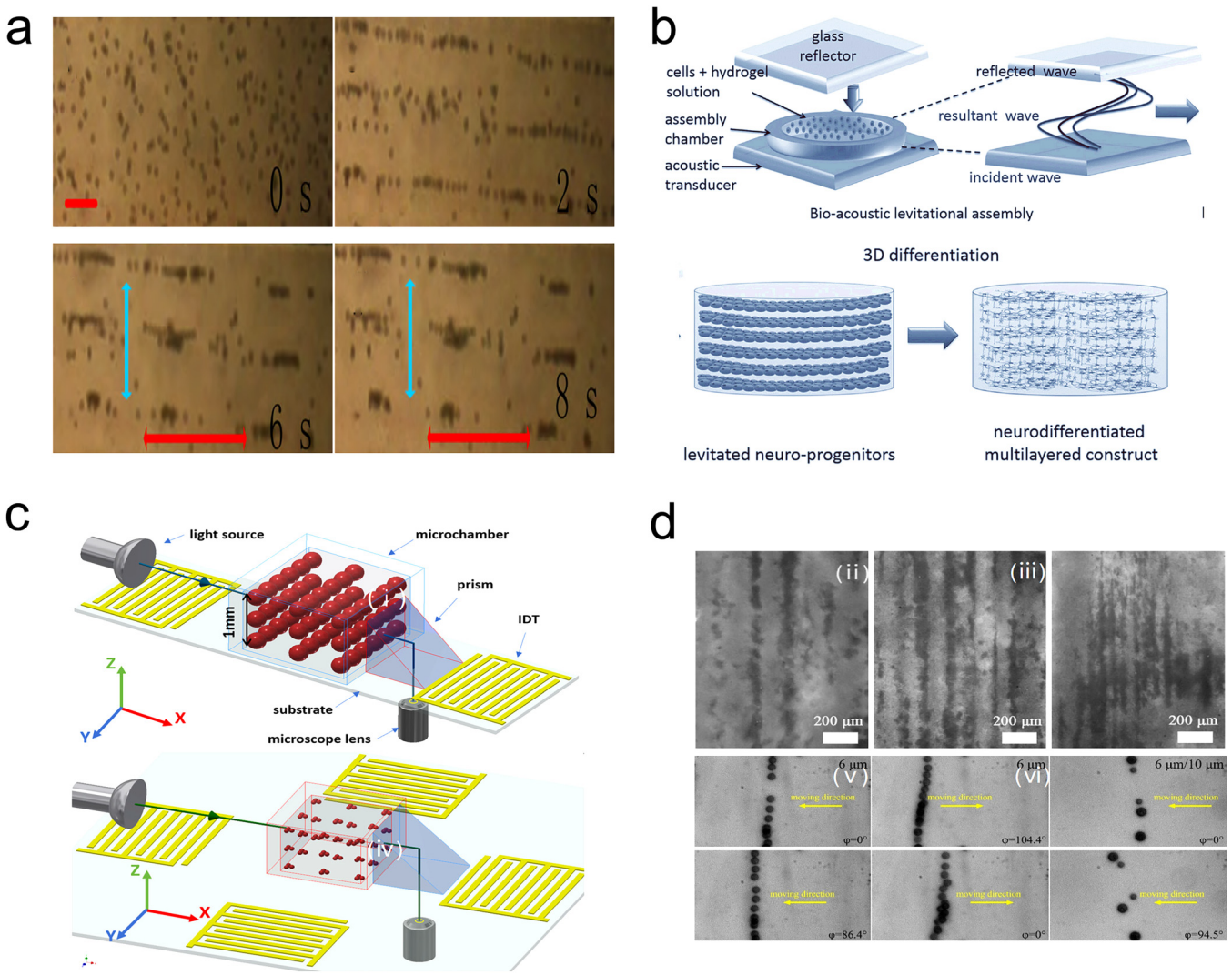

FIG. 10. (a) Picture of the process of patterning particles into 2D patterns, and the direction of the blue arrow coincides with the direction of SAW propagation. Reproduced with permission from Zheng *et al.*, Sens. Actuators A **284**, 168–171 (2018). Copyright 2018 Elsevier B.V.[116] (b) Schematic of acoustic levitation. The suspension containing embryonic stem cells is introduced into the suspension chamber and thrombin is added for the gelation process. The transducer is activated to generate acoustic waves that drive the cells to form a 3D multilayer structure. Reproduced with permission from Bouyer *et al.*, Adv. Mater. **28**(1), 161–167 (2016). Copyright 2018 John Wiley & Sons.[117] (c) Schematic diagram of the experimental setup for 3D lines formed by microparticles with a diameter of 10 μm, and the illustration of a 3D structure similar to a crystal lattice. Reproduced with permission from Nguyen *et al.*, Appl. Phys. Lett. **112**(21), 213507 (2018). Copyright 2018 AIP Publishing LLC.[119] (d) Particle patterns at different SAW frequencies [(i) 12.2, (ii) 24.0, and (iii) 42.2 MHz] and the change in position of two different size particles after changing the phase angle. Reproduced with permission from Tao *et al.*, Sens. Actuators B **299**, 126991 (2019). Copyright 2019 Elsevier B.V.[120]

Although magnetic patterning has low cost and high efficiency, magnetic beads need to be used to label cells that lack paramagnetic or diamagnetic properties. Acoustic microfluidics is widely used because of its biocompatibility and non-labeling. Finite acoustic pressure nodes are created within the microchannel by acoustic waves, and the particles in the microchannel can be arranged in an orderly manner to achieve precise particle manipulation, which is acoustic patterning. The biocompatibility of acoustic waves enables acoustic microfluidics to address many biological challenges, such as tissue engineering. The speed of acoustic patterning is faster compared to other methods.

F. Acoustic-based heating

Acoustic surface waves propagate along the surface of the piezoelectric substrate, and in this process, part of the acoustic energy

undergoes energy conversion to generate thermal energy due to vibration damping present in the propagation path. This phenomenon is commonly called the heating effect. The mechanism of the acoustic thermal effect is still unclear. In order to investigate and apply the acoustic thermal effect better, a theoretical model based on multi-scale perturbation was proposed by Das *et al.*[122] Research has proved that the temperature rise of the acoustic wave depends on the energy density of the acoustic wave and the conversion of acoustic energy to internal energy. The acoustic wave temperature can be raised by increasing the size of the system and the frequency of SAW.

Ha *et al.* investigated the heating of polydimethylsiloxane (PDMS) under the effect of high-frequency acoustic waves and successfully achieved the temperature control of polymerase chain reaction (PCR) microreactions.[123] In this experiment, they achieved amplification of a 134bp DNA amplicon in 3 min. The SAW was refracted into the PDMS-fabricated microchannel in the form of a leakage wave that heated the microchannel uniformly and rapidly. The CFPCR chip is shown in Fig. 11(a)(i); two IDTs used for denaturation and annealing/extension were deposited on the substrate. The advantage of this device is that it can rapidly perform DNA amplification and continuously complete the entire experiment in a closed microchannel, thus avoiding cross-contamination of samples. By altering the shape of the IDT, different waveforms could be generated at multiple positions. The penetration depth at various IDTs and different drive frequencies are shown in Figs. 11(a)(ii)–11(a)(v).

Meng *et al.* utilized temperature-sensitive liposomes (TSL) for drug release with the effects of micro high intensity focused ultrasound (MHIFU) investigated, when MHIFU manipulates the cellular drug.[124] The device is shown in Fig. 11(b), and focused acoustic energy was generated by a single element unidirectional transducer (SPIDT). MHIFU was applied to the TSL, the encapsulated drug (Adriamycin DOX) was released from it due to the thermal effect and the mechanical effect, and then the drug was internalized by 4T1. It was demonstrated that the thermal and mechanical effects of SAW acted synergistically. The lipid layer of TSL was melted by the thermal effect, while the mechanical effect like acoustic flow caused DOX to homogeneously mix and agitate, further improving the odds of collision between DOX and cells.

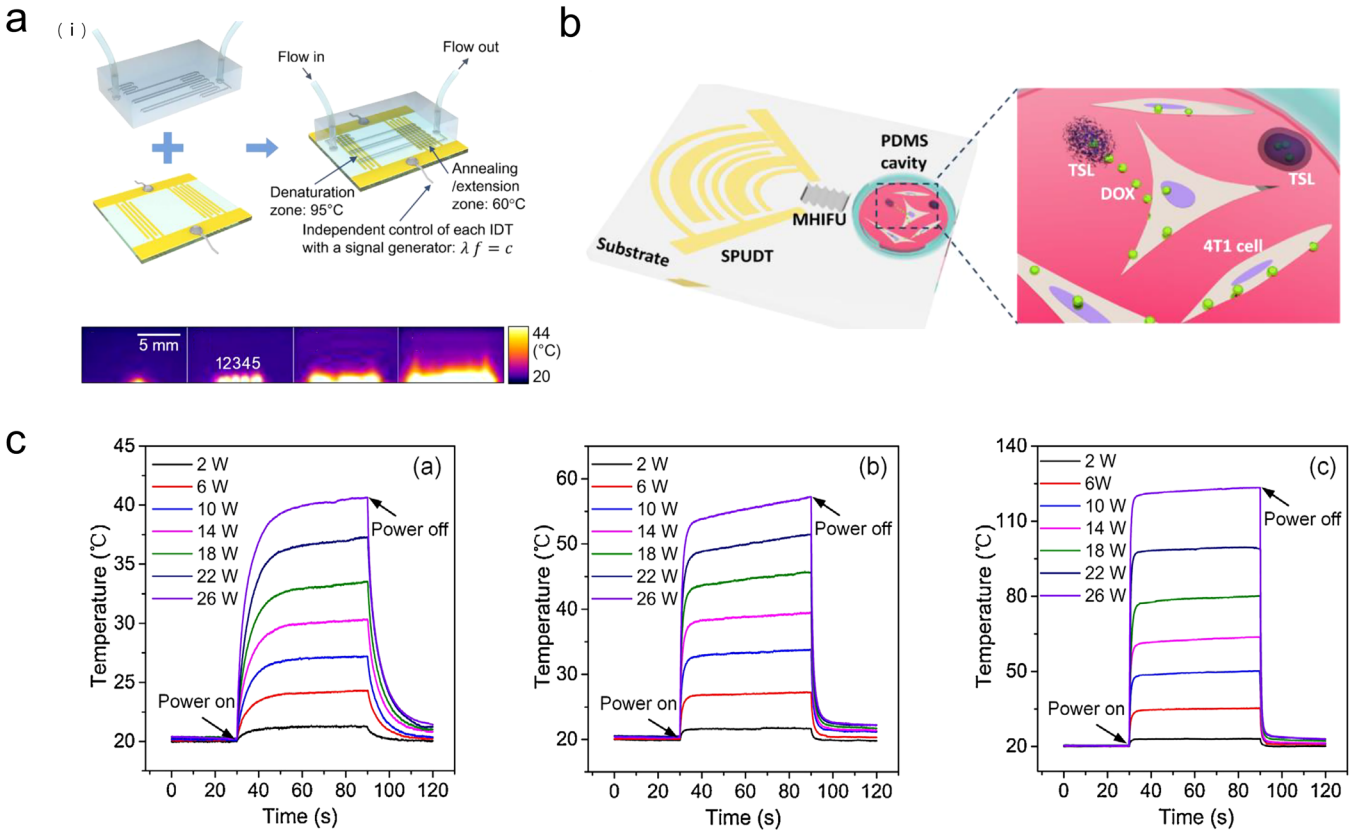

FIG. 11. (a) Schematic diagram of the CFPCR chip and the infrared images of penetration depth [(ii) the focused IDT of 128.5 MHz,;(iii) the slanted IDT of 36, 32, 28, 24, and 20 MHz; (iv) the straight IDT of 16.1 MHz; and (v) the straight IDT of 9.8 MHz). From Ha *et al.*, Sci. Rep. **5**(1), 11851 (2015). Copyright 2015 Author(s), licensed under a Creative Commons Attribution (CC BY) License.[123] (b) Schematic of the MHIFU device and TSL release. From Meng *et al.*, Theranostics **5**(11), 1203–1213 (2015). Copyright 2015 Author(s), licensed under a Creative Commons Attribution (CC BY) License.[124] (c) Diagram of temperature comparison of three different thin-film SAW devices. Reproduced with permission from Wang *et al.*, Sens. Actuators A **318**, 112508 (2021). Copyright 2021 Elsevier B.V.[126]

TABLE II. Typical techniques and applications of acoustic microfluidics.

Application of acoustic microfluidics		Application	Mechanism	Advantages
Acoustic sorting	SAW-based	• Cells and droplets sorting • Cell-based diagnosis and therapy	Acoustic radiation force	• High sorting rate • High throughput
	BAW-based			• Low working frequency • The ability to sort large size particles
Acoustic mixing		• Synthetic bioparticles • Droplet encapsulation • Fluid mixing	Acoustic streaming; Bubbles	• High mixing efficiency • Applicable to low R_e numbers
Acoustic atomization		• Drug delivery • Mass spectrometry • Medical inhalator	Acoustic beam interaction with acoustic waves	• High-energy transfer efficiency • Low input energy (1–3 w)
Trapping and release		• Cell studies • Droplet detection	Acoustic radiation force	• Biocompatibility • Manufacturing convenience
Acoustic patterning		• Tissue engineering • 3D biomimetic tissue structures • Microarrays	Acoustic radiation force and drug force	• Fast assembly speed • Biocompatibility
Acoustic-based heating		• Liquid heating • Drug release by thermal	Acoustic thermal effect	• Localized energy • Non-invasive • Precise temperature control

To solve the limitations of unidirectional droplet sorting, bidirectional droplet sorting is used to improve the versatility of the sorting system and to precisely control the position of droplets. A novel droplet sorter driven by the acoustic heating effect was introduced by Park *et al.*[125] The sorting system consisted of an acoustic thermal heater and a microfluidic chip, which was composed of a piezoelectric substrate, a slanted finger IDT deposited on the substrate, and PDMS microchannels. The PDMS microchannels consisted of three inlets and multiple outlets. The heat was transferred to the moving droplet above the acoustic heater by thermal diffusion. As a result, the droplet was pushed laterally along the interface by the thermocapillary effect. Because of the action of surfactants, the interfacial tension varies along the surface of the droplet at the temperature gradient, resulting in the formation of Marangoni microvortices inside and outside the droplet, and these microvortices caused the capillary droplets to move toward the low-temperature region.

Common $LiNbO_3$ substrates are easily damaged under strong thermal shock and difficult to integrate with other microfluidic devices. To solve this problem, a thin-film SAW-based microheater was proposed by Wang *et al.* After comparing with several thin-film materials, AlN/Si was selected.[126] As shown in Fig. 11(c), the AlN/Si device based on SAW has the best heating level at the same power and good temperature stability. Due to a longer SAW attenuation length and a smaller size of PDMS chamber, the fluid streaming and mixing can be enhanced and the temperature uniformity could be improved. The experiment proved that the device could accurately control the temperature of the samples with excellent reliability.

In general, the acoustic thermal effect produced by acoustic waves on microfluidics may damage cells, which makes the practical application of acoustic microfluidics to have limitations. It has been demonstrated that the acoustic thermal effect can also be exploited. According to the available research studies, compared with the traditional heating method, the method of microfluidic temperature control based on the acoustothermal effect has the advantage of miniaturization of the device, simplicity, and short response time, which has a broad application prospect and deserves further research. Table II summarizes typical techniques and applications of acoustic microfluidics.

V. CONCLUSION AND FUTURE PERSPECTIVE

This article reviews the current acoustic microfluidics techniques and briefly describes the partial applications of acoustic microfluidics according to their different functions. Acoustic microfluidics has been widely applied in various fields such as biochemistry and medicine, including cell separation, reagent mixing, drug delivery, immediate testing, clinical diagnosis, and cell patterning. Compared with traditional methods previously used for these applications, acoustic microfluidics has the advantages of

miniaturization, non-contact, and biocompatibility. As a result, it has been growing rapidly to replace traditional tools.

Most acoustic microfluidics utilize acoustic radiation force and acoustic streaming generated by acoustic waves to perform the majority of functions. In general, acoustic radiation force, especially primary acoustic radiation force, is the main factor for acoustic-based microparticle manipulation, while acoustic streaming is considered to interfere with what would otherwise be predictable motion.[127] Therefore, exploring methods to minimize the influence of acoustics is useful to improve the precision of microparticle manipulation. Meanwhile, when using acoustic microfluidics for cell manipulation, the thermal effect of the acoustic wave may damage the cell viability. The thermal effect of the acoustic wave should be further investigated, although this phenomenon already has a variety of applications.

Currently, acoustic microfluidics is mainly used to process submillimeter- or sub-micrometer-scale objects. The control of sub-nanometer-scale objects is critically important for the development of acoustic microfluidics. In terms of acoustic frequencies, the majority of frequencies used are generally at a low level, which varies between 1 and 10 KHz, but high-frequency acoustic microfluidics is rarely explored. The application of GHz frequency is of great significance to the improvement of the accuracy and efficiency of acoustic microfluidics. Similarly, the efficiency of acoustic microfluidics can also be improved by exploring the new geometry of IDT and the geometry of microchannels.

Acoustic microfluidics can achieve acoustic manipulation in multiple degrees of freedom, including manipulation in the x axis, y axis, and z axis.[128] However, the z axis manipulation is not as flexible as other axes; thus, its flexibility needs to be improved. To make acoustic-based methods better for applications, the accuracy of z axis control also needs to be further improved.

At present, most acoustic-based cell and microparticle patterning are static, limited to the physical definition of the standing wave field to form a fixed pattern, and the microparticles and cells cannot be manipulated individually. In order to better apply acoustic microfluidics to the field of bioengineering applications, it is necessary to realize cell patterns of arbitrary shapes and allow the use of acoustics to control individual cells. The arrays of emitters are capable of creating dynamic and complex acoustic fields, allowing for the individual and simultaneous manipulation of multiple objects. Individual objects can be controlled by combining 3D field devices with microscopy and analysis. Holograms have high-phase fidelity but are generally used to generate static acoustic fields because they lack dynamic flexibility.[129–131] In recent research advances, the more complex dynamic ultrasound fields can be generated by combining the arrays of emitters and the holograms, enabling selective cell manipulation.

Furthermore, the currently developed acoustic microfluidic devices usually need to be integrated with other large-scale devices, which are usually more expensive, and the complexity of the system is increased. To enable the acoustic microfluidic equipment to be widely used, it is essential to construct an integrated device that can accomplish the experimental process completely from the beginning to the end and realize the miniaturization of the integrated device. Etching and soft lithography are the common techniques adopted to fabricate microfluidic chips. Etching is a technique for microfabrication using photoresists, masks, and UV light and is widely applied to silicon, glass, and quartz substrates.[132] Unlike etching, soft lithography is suitable for polymers, especially PDMS.[133,134] Traditional techniques for fabricating microfluidics require a clean room environment, and the iterative steps are usually required, resulting in significant costs. In addition, each design iteration requires printing a new photolithography mask and UV lithography to make a new master, which is more complex and time-consuming.[135] It is not conducive to the innovation and development of microfluidic technology. To shorten the fabrication time and reduce the fabrication costs of acoustic microfluidic devices, it is necessary to explore simpler and cheaper manufacturing technologies, such as 3D printing. Other substrate materials can also be explored to further reduce manufacturing costs, such as the use of piezoelectric films. At the same time, disposable components with fixed geometric shapes should also become a development trend.

ACKNOWLEDGMENTS

The authors wish to acknowledge the funding provided by the National Natural Science Foundation of China (NNSFC) (Project No. 61803323), the Natural Science Foundation of Shandong Province (Project No. ZR2019BF049), and the Joint fund of Science and Technology Department of Liaoning Province and State Key Laboratory of Robotics (Project No. 2021-KF-22-03).

AUTHOR DECLARATIONS

Conflict of Interest

The authors have no conflicts to disclose.

Author Contributions

Yue Li: Writing – original draft (equal). **Shuxiang Cai:** Supervision (equal); writing – review & editing (equal). **Honglin Shen:** Writing – original draft (equal). **Yibao Chen:** Writing – review & editing (equal). **Zhixing Ge:** Supervision (equal); writing – review & editing (equal). **Wenguang Yang:** Funding acquisition (equal); supervision (equal); writing – review & editing (equal).

DATA AVAILABILITY

Data sharing is not applicable to this article as no new data were created or analyzed in this study.

REFERENCES

[1]P. Supramaniam, O. Ces, and A. Salehi-Reyhani, "Microfluidics for artificial life: Techniques for bottom-Up synthetic biology," Micromachines **10**(5), 299 (2019).
[2]W.-L. Chou *et al.*, "Recent advances in applications of droplet microfluidics," Micromachines **6**(9), 1249–1271 (2015).
[3]Y. Liu and X. Jiang, "Why microfluidics? Merits and trends in chemical synthesis," Lab Chip **17**(23), 3960–3978 (2017).
[4]S. Mashaghi *et al.*, "Droplet microfluidics: A tool for biology, chemistry and nanotechnology," Trends Anal. Chem. **82**, 118–125 (2016).
[5]E. K. Sackmann, A. L. Fulton, and D. J. Beebe, "The present and future role of microfluidics in biomedical research," Nature **507**(7491), 181–189 (2014).

[6]A. Karimi, S. Yazdi, and A. M. Ardekani, "Hydrodynamic mechanisms of cell and particle trapping in microfluidics," Biomicrofluidics **7**(2), 021501 (2013).
[7]N. Lewpiriyawong, C. Yang, and Y. C. Lam, "Continuous sorting and separation of microparticles by size using AC dielectrophoresis in a PDMS microfluidic device with 3-D conducting PDMS composite electrodes," Electrophoresis **31**(15), 2622–2631 (2010).
[8]A. H. C. Ng *et al.*, "Digital microfluidic magnetic separation for particle-based immunoassays," Anal. Chem. **84**(20), 8805–8812 (2012).
[9]H. Yang and M. A. M. Gijs, "Micro-optics for microfluidic analytical applications," Chem. Soc. Rev. **47**(4), 1391–1458 (2018).
[10]P. Li *et al.*, "Detachable acoustophoretic system for fluorescence-activated sorting at the single-droplet level," Anal. Chem. **91**(15), 9970–9977 (2019).
[11]M. A. Burguillos *et al.*, "Microchannel acoustophoresis does not impact survival or function of microglia, leukocytes or tumor cells," PLoS One **8**(5), e64233 (2013).
[12]D. L. Miller *et al.*, "Overview of therapeutic ultrasound applications and safety considerations," J. Ultrasound Med. **31**(4), 623–634 (2012).
[13]C. S. Centner *et al.*, "Ultrasound-induced molecular delivery to erythrocytes using a microfluidic system," Biomicrofluidics **14**(2), 024114 (2020).
[14]D. N. Ankrett *et al.*, "The effect of ultrasound-related stimuli on cell viability in microfluidic channels," J. Nanobiotechnol. **11**(1), 20 (2013).
[15]Lord Rayleigh, "On waves propagated along the plane surface of an elastic solid," Proc. London Math. Soc. **s1-17**(1), 4–11 (1885).
[16]R. M. White and F. W. Voltmer, "Direct piezoelectric coupling to surface elastic waves," Appl. Phys. Lett. **7**, 314 (1965).
[17]C. Wyatt Shields IV, C. D. Reyes, and G. P. López, "Microfluidic cell sorting: A review of the advances in the separation of cells from debulking to rare cell isolation," Lab Chip **15**(5), 1230–1249 (2015).
[18]Y. Bian *et al.*, "Acoustofluidic waveguides for localized control of acoustic wavefront in microfluidics," Microfluid. Nanofluid. **21**(8), 132 (2017).
[19]L. V. King, "On the acoustic radiation pressure on spheres," Proc. R. Soc. London, A **147**(861), 212–240 (1934).
[20]L. P. Gor'kov, "On the forces acting on a small particle in an acoustical field in an ideal fluid," Sov. Phys. Dokl. **6**(1), 773 (1962).
[21]G. Destgeer *et al.*, "Adjustable, rapidly switching microfluidic gradient generation using focused travelling surface acoustic waves," Appl. Phys. Lett. **104**(2), 023506 (2014).
[22]V. Bjerknes, *Fields of Force: Supplementary Lectures, Applications to Meteorology; A Course of Lectures in Mathematical Physics Delivered December 1 to 23, 1905* (Columbia University Press, 1906).
[23]M. A. H. Weiser, R. E. Apfel, and E. A. Neppiras, "Interparticle forces on red cells in a standing wave field," Acta Acust. **56**(2), 114–119 (1984).
[24]L. A. Crum, "Bjerknes forces on bubbles in a stationary sound field," J. Acoust. Soc. Am. **57**(6), 1363–1370 (1975).
[25]A. Doinikov, *Recent Research Developments in Acoustics* (Transworld Research Network, Trivandrum, Kerala, India, 2003), Vol. 1, Chap. 3; available at https://www.researchgate.net/publication/235345891_Acoustic_radiation_forces_Classical_theory_and_recent_advances.
[26]R. Habibi, C. Devendran, and A. Neild, "Trapping and patterning of large particles and cells in a 1D ultrasonic standing wave," Lab Chip **17**(19), 3279–3290 (2017).
[27]A. R. Mohapatra, S. Sepehrirahnama, and K.-M. Lim, "Experimental measurement of interparticle acoustic radiation force in the Rayleigh limit," Phys. Rev. E **97**(5), 053105 (2018).
[28]D. Saeidi *et al.*, "A quantitative study of the secondary acoustic radiation force on biological cells during acoustophoresis," Micromachines **11**(2), 152 (2020).
[29]T. Laurell, F. Petersson, and A. Nilsson, "Chip integrated strategies for acoustic separation and manipulation of cells and particles," Chem. Soc. Rev. **36**(3), 492–506 (2007).
[30]T. Masudo and T. Okada, "Particle separation with ultrasound radiation force," Curr. Anal. Chem. **2**(2), 213–227 (2006).
[31]J. Jeon *et al.*, "Acoustically excited oscillating bubble on a flexible structure and its energy-harvesting capability," Int. J. Precis. Eng. Manuf. Green Technol. **6**(3), 531–537 (2019).
[32]A. T. Chwang and T. Y.-T. Wu, "Hydromechanics of low-Reynolds-number flow. Part 2. Singularity method for stokes flows," J. Fluid Mech. **67**(4), 787–815 (1975).
[33]A. Lenshof *et al.*, "Acoustofluidics 5: Building microfluidic acoustic resonators," Lab Chip **12**(4), 684–695 (2012).
[34]F. Garofalo, T. Laurell, and H. Bruus, "Performance study of acoustophoretic microfluidic silicon-glass devices by characterization of material- and geometry-dependent frequency spectra," Phys. Rev. Appl. **7**(5), 054026 (2017).
[35]A. Fornell *et al.*, "Fabrication of silicon microfluidic chips for acoustic particle focusing using direct laser writing," Micromachines **11**(2), 113 (2020).
[36]M. C. Jo and R. Guldiken, "Effects of polydimethylsiloxane (PDMS) microchannels on surface acoustic wave-based microfluidic devices," Microelectron. Eng. **113**, 98–104 (2014).
[37]Z. Zhu *et al.*, "A versatile bonding method for PDMS and SU-8 and its application towards a multifunctional microfluidic device," Micromachines **7**(12), 230 (2016).
[38]Z. Wu *et al.*, "Medical micro/nanorobots in complex media," Chem. Soc. Rev. **49**(22), 8088–8112 (2020).
[39]D. J. Collins, A. Neild, and Y. Ai, "Highly focused high-frequency travelling surface acoustic waves (SAW) for rapid single-particle sorting," Lab Chip **16**(3), 471–479 (2016).
[40]M. Weiß *et al.*, "Multiharmonic frequency-chirped transducers for surface-acoustic-wave optomechanics," Phys. Rev. Appl. **9**(1), 014004 (2018).
[41]G. P. Gautam *et al.*, "Simple and inexpensive micromachined aluminum microfluidic devices for acoustic focusing of particles and cells," Anal. Bioanal. Chem. **410**(14), 3385–3394 (2018).
[42]I. Leibacher, P. Reichert, and J. Dual, "Microfluidic droplet handling by bulk acoustic wave (BAW) acoustophoresis," Lab Chip **15**(13), 2896–2905 (2015).
[43]H. Pereira *et al.*, "Fluorescence activated cell-sorting principles and applications in microalgal biotechnology," Algal Res. **30**, 113–120 (2018).
[44]M. E. Warkiani *et al.*, "Large-volume microfluidic cell sorting for biomedical applications," Annu. Rev. Biomed. Eng. **17**(1), 1–34 (2015).
[45]S. Basu *et al.*, "Purification of specific cell population by fluorescence activated cell sorting (FACS)," JoVE **41**, e1546 (2010).
[46]L. Liu *et al.*, "Isolation of skeletal muscle stem cells by fluorescence-activated cell sorting," Nat. Protoc. **10**(10), 1612–1624 (2015).
[47]L. Schmid, D. A. Weitz, and T. Franke, "Sorting drops and cells with acoustics: Acoustic microfluidic fluorescence-activated cell sorter," Lab Chip **14**(19), 3710–3718 (2014).
[48]X. Ding *et al.*, "Standing surface acoustic wave (SSAW) based multichannel cell sorting," Lab Chip **12**(21), 4228–4231 (2012).
[49]W. L. Ung *et al.*, "Enhanced surface acoustic wave cell sorting by 3D microfluidic-chip design," Lab Chip **17**(23), 4059–4069 (2017).
[50]P. Ohlsson *et al.*, "Acoustic impedance matched buffers enable separation of bacteria from blood cells at high cell concentrations," Sci. Rep. **8**(1), 9156 (2018).
[51]A. Shamloo and M. Boodaghi, "Design and simulation of a microfluidic device for acoustic cell separation," Ultrasonics **84**, 234–243 (2018).
[52]V. Plaks, D. C. Koopman, and Z. Werb, "Circulating tumor cells," Science **341**(6151), 1186–1188 (2013).
[53]K. Pantel and M. R. Speicher, "The biology of circulating tumor cells," Oncogene **35**(10), 1216–1224 (2016).
[54]K. Wang *et al.*, "Sorting of tumour cells in a microfluidic device by multi-stage surface acoustic waves," Sens. Actuators B **258**, 1174–1183 (2018).
[55]Y. Zhou, Z. Ma, and Y. Ai, "Hybrid microfluidic sorting of rare cells based on high throughput inertial focusing and high accuracy acoustic manipulation," RSC Adv. **9**(53), 31186–31195 (2019).
[56]M. Tenje *et al.*, "Particle manipulation methods in droplet microfluidics," Anal. Chem. **90**(3), 1434–1443 (2018).
[57]C. Devendran, I. Gralinski, and A. Neild, "Separation of particles using acoustic streaming and radiation forces in an open microfluidic channel," Microfluid. Nanofluid. **17**(5), 879–890 (2014).
[58]J. Lei *et al.*, "Two-dimensional concentration of microparticles using bulk acousto-microfluidics," Appl. Phys. Lett. **116**(3), 033104 (2020).

[59]P. Dow *et al.*, "Acoustic separation in plastic microfluidics for rapid detection of bacteria in blood using engineered bacteriophage," Lab Chip **18**(6), 923–932 (2018).
[60]M. Janczuk *et al.*, "Bacteriophage-based bioconjugates as a flow cytometry probe for fast bacteria detection," Bioconjugate Chem. **28**(2), 419–425 (2017).
[61]A. Adan *et al.*, "Flow cytometry: Basic principles and applications," Crit. Rev. Biotechnol. **37**(2), 163–176 (2017).
[62]S. F. Ibrahim and G. van den Engh, "Flow cytometry and cell sorting," in *Cell Separation: Fundamentals, Analytical and Preparative Methods*, edited by A. Kumar, I. Y. Galaev, and B. Mattiasson (Springer, Berlin, 2007), pp. 19–39.
[63]S. R. Delwiche, T. C. Pearson, and D. L. Brabec, "High-speed optical sorting of soft wheat for reduction of deoxynivalenol," Plant Dis. **89**(11), 1214–1219 (2005).
[64]R.-J. Yang *et al.*, "Micro-magnetofluidics in microfluidic systems: A review," Sens. Actuators B **224**, 1–15 (2016).
[65]M. Kakuta, F. G. Bessoth, and A. Manz, "Microfabricated devices for fluid mixing and their application for chemical synthesis," Chem. Rec. **1**(5), 395–405 (2001).
[66]A. Karimipour *et al.*, "Thermal conductivity enhancement via synthesis produces a new hybrid mixture composed of copper oxide and multi-walled carbon nanotube dispersed in water: Experimental characterization and artificial neural network modeling," Int. J. Thermophys. **41**(8), 116 (2020).
[67]C.-H. Choi, D. A. Weitz, and C.-S. Lee, "One step formation of controllable complex emulsions: From functional particles to simultaneous encapsulation of hydrophilic and hydrophobic agents into desired position," Adv. Mater. **25**(18), 2536–2541 (2013).
[68]Y. Li *et al.*, "Synthesis of new dihybrid nanofluid of TiO_2/MWCNT in water-ethylene glycol to improve mixture thermal performance: Preparation, characterization, and a novel correlation via ANN based on orthogonal distance regression algorithm," J. Therm. Anal. Calorim. **144**(6), 2587–2603 (2021).
[69]H. Ahmed *et al.*, "Surface acoustic wave-based micromixing enhancement using a single interdigital transducer," Appl. Phys. Lett. **114**(4), 043702 (2019).
[70]J. Nam, W. S. Jang, and C. S. Lim, "Micromixing using a conductive liquid-based focused surface acoustic wave (CL-FSAW)," Sens. Actuators B **258**, 991–997 (2018).
[71]J. Nam and C. S. Lim, "Micromixing using swirling induced by three-dimensional dual surface acoustic waves (3D-dSAW)," Sens. Actuators B **255**, 3434–3440 (2018).
[72]M. R. Rasouli and M. Tabrizian, "An ultra-rapid acoustic micromixer for synthesis of organic nanoparticles," Lab Chip **19**(19), 3316–3325 (2019).
[73]T. Kong *et al.*, "Droplet based microfluidic fabrication of designer microparticles for encapsulation applications," Biomicrofluidics **6**(3), 034104 (2012).
[74]M. T. Chung *et al.*, "Deterministic droplet-based co-encapsulation and pairing of microparticles via active sorting and downstream merging," Lab Chip **17**(21), 3664–3671 (2017).
[75]D. J. Collins *et al.*, "Surface acoustic waves for on-demand production of picoliter droplets and particle encapsulation," Lab Chip **13**(16), 3225–3231 (2013).
[76]M. Wierucka and M. Biziuk, "Application of magnetic nanoparticles for magnetic solid-phase extraction in preparing biological, environmental and food samples," Trends Anal. Chem. **59**, 50–58 (2014).
[77]W. J. Stark *et al.*, "Industrial applications of nanoparticles," Chem. Soc. Rev. **44**(16), 5793–5805 (2015).
[78]R. Sridhar *et al.*, "Electrosprayed nanoparticles and electrospun nanofibers based on natural materials: Applications in tissue regeneration, drug delivery and pharmaceuticals," Chem. Soc. Rev. **44**(3), 790–814 (2015).
[79]Z. Wu, S. Yang, and W. Wu, "Shape control of inorganic nanoparticles from solution," Nanoscale **8**(3), 1237–1259 (2016).
[80]N. H. An Le *et al.*, "Ultrafast star-shaped acoustic micromixer for high throughput nanoparticle synthesis," Lab Chip **20**(3), 582–591 (2020).
[81]A. Pourabed *et al.*, "High throughput acoustic microfluidic mixer controls self-assembly of protein nanoparticles with tuneable sizes," J. Colloid Interface Sci. **585**, 229–236 (2021).
[82]H. Bockelmann, V. Heuveline, and D. P. J. Barz, "Optimization of an electrokinetic mixer for microfluidic applications," Biomicrofluidics **6**(2), 024123 (2012).
[83]X. Chen and L. Zhang, "A review on micromixers actuated with magnetic nanomaterials," Microchim. Acta **184**(10), 3639–3649 (2017).
[84]B. Xu *et al.*, "Thermal mixing of two miscible fluids in a T-shaped microchannel," Biomicrofluidics **4**(4), 044102 (2010).
[85]W. Zhao *et al.*, "Rapid mixing by turbulent-like electrokinetic microflow," Chem. Eng. Sci. **165**, 113–121 (2017).
[86]T. C. Carvalho and J. T. McConville, "The function and performance of aqueous aerosol devices for inhalation therapy," J. Pharm. Pharmacol. **68**(5), 556–578 (2016).
[87]A. Qi *et al.*, "Miniature inhalation therapy platform using surface acoustic wave microfluidic atomization," Lab Chip **9**(15), 2184–2193 (2009).
[88]T. P. Forbes, "Rapid detection and isotopic measurement of discrete inorganic samples using acoustically actuated droplet ejection and extractive electrospray ionization mass spectrometry," Rapid Commun. Mass Spectrom. **29**(1), 19–28 (2015).
[89]M. Yousefi *et al.*, "CFD simulation of aerosol delivery to a human lung via surface acoustic wave nebulization," Biomech. Model. Mechanobiol. **16**(6), 2035–2050 (2017).
[90]A. Winkler *et al.*, "SAW-based fluid atomization using mass-producible chip devices," Lab Chip **15**(18), 3793–3799 (2015).
[91]Y. N. Cheung, N. T. Nguyen, and T. N. Wong, "Low-frequency acoustic atomization with oscillatory flow around micropillars in a microfluidic device," Appl. Phys. Lett. **105**(14), 144103 (2014).
[92]A. Yabe *et al.*, "A self-converging atomized mist spray device using surface acoustic wave," Microfluid. Nanofluid. **17**(4), 701–710 (2014).
[93]P. Sharma *et al.*, "Emerging trends in the novel drug delivery approaches for the treatment of lung cancer," Chem. Biol. Interact. **309**, 108720 (2019).
[94]V. Ramalingam *et al.*, "Target delivery of doxorubicin tethered with PVP stabilized gold nanoparticles for effective treatment of lung cancer," Sci. Rep. **8**(1), 3815 (2018).
[95]R. B. Dunne and S. Shortt, "Comparison of bronchodilator administration with vibrating mesh nebulizer and standard jet nebulizer in the emergency department," Am. J. Emerg. Med. **36**(4), 641–646 (2018).
[96]Y.-L. Song, C.-H. Cheng, and M. K. Reddy, "Numerical analysis of ultrasonic nebulizer for onset amplitude of vibration with atomization experimental results," Water **13**(14), 1972 (2021).
[97]V. C. Galindo-Filho *et al.*, "A mesh nebulizer is more effective than jet nebulizer to nebulize bronchodilators during non-invasive ventilation of subjects with COPD: A randomized controlled trial with radiolabeled aerosols," Respir. Med. **153**, 60–67 (2019).
[98]C. Cortez-Jugo *et al.*, "Pulmonary monoclonal antibody delivery via a portable microfluidic nebulization platform," Biomicrofluidics **9**(5), 052603 (2015).
[99]C. Lopez-Causape *et al.*, "Clonal dissemination, emergence of mutator lineages and antibiotic resistance evolution in *Pseudomonas aeruginosa* cystic fibrosis chronic lung infection," PLoS One **8**(8), e71001 (2013).
[100]R. M. Dedrick *et al.*, "Engineered bacteriophages for treatment of a patient with a disseminated drug-resistant *Mycobacterium abscessus*," Nat. Med. **25**(5), 730–733 (2019).
[101]N. Principi, E. Silvestri, and S. Esposito, "Advantages and limitations of bacteriophages for the treatment of bacterial infections," Front. Pharmacol. **10**, 513 (2019).
[102]K. Abdelkader *et al.*, "The preclinical and clinical progress of bacteriophages and their lytic enzymes: The parts are easier than the whole," Viruses **11**(2), 96 (2019).
[103]S. Garcia-Santamarina *et al.*, "A lytic polysaccharide monooxygenase-like protein functions in fungal copper import and meningitis," Nat. Chem. Biol. **16**(3), 337–344 (2020).
[104]S. Marqus *et al.*, "High frequency acoustic nebulization for pulmonary delivery of antibiotic alternatives against *Staphylococcus aureus*," Eur. J. Pharm. Biopharm. **151**, 181–188 (2020).

[105]H. Ahmed *et al.*, "A novel acoustomicrofluidic nebulization technique yielding new crystallization morphologies," Adv. Mater. **30**(3), 1602040 (2018).
[106]K. S. Wong *et al.*, "*In situ* generation of plasma-activated aerosols via surface acoustic wave nebulization for portable spray-based surface bacterial inactivation," Lab Chip **20**(10), 1856–1868 (2020).
[107]J. H. Jung *et al.*, "On-demand droplet capture and release using microwell-assisted surface acoustic waves," Anal. Chem. **89**(4), 2211–2215 (2017).
[108]R. W. Rambach *et al.*, "Droplet trapping and fast acoustic release in a multi-height device with steady-state flow," Lab Chip **17**(20), 3422–3430 (2017).
[109]D. M. Pegtel and S. J. Gould, "Exosomes," Annu. Rev. Biochem. **88**(1), 487–514 (2019).
[110]R. Linares *et al.*, "High-speed centrifugation induces aggregation of extracellular vesicles," J. Extracell. Vesicles **4**(1), 29509 (2015).
[111]R. Habibi *et al.*, "Exosome trapping and enrichment using a sound wave activated nano-sieve (SWANS)," Lab Chip **20**(19), 3633–3643 (2020).
[112]H. Ahmed *et al.*, "Sheathless focusing and separation of microparticles using tilted-angle traveling surface acoustic waves," Anal. Chem. **90**(14), 8546–8552 (2018).
[113]V. Narayanamurthy *et al.*, "Microfluidic hydrodynamic trapping for single cell analysis: Mechanisms, methods and applications," Anal. Methods **9**(25), 3751–3772 (2017).
[114]N. Ashammakhi *et al.*, "Bioinks and bioprinting technologies to make heterogeneous and biomimetic tissue constructs," Mater. Today Bio **1**, 100008 (2019).
[115]Y. Yang *et al.*, "Recent progress in biomimetic additive manufacturing technology: From materials to functional structures," Adv. Mater. **30**(36), 1706539 (2018).
[116]T. Zheng *et al.*, "Patterning microparticles into a two-dimensional pattern using one column standing surface acoustic waves," Sens. Actuators A **284**, 168–171 (2018).
[117]C. Bouyer *et al.*, "A bio-acoustic levitational (BAL) assembly method for engineering of multilayered, 3D brain-like constructs, using human embryonic stem cell derived neuro-progenitors," Adv. Mater. **28**(1), 161–167 (2016).
[118]S. M. Naseer *et al.*, "Surface acoustic waves induced micropatterning of cells in gelatin methacryloyl (GelMA) hydrogels," Biofabrication **9**(1), 015020 (2017).
[119]T. D. Nguyen *et al.*, "Patterning and manipulating microparticles into a three-dimensional matrix using standing surface acoustic waves," Appl. Phys. Lett. **112**(21), 213507 (2018).
[120]X. Tao *et al.*, "3D patterning/manipulating microparticles and yeast cells using ZnO/Si thin film surface acoustic waves," Sens. Actuators B **299**, 126991 (2019).
[121]W. Yang *et al.*, "Recent advance in cell patterning techniques: Approaches, applications and future prospects," Sens. Actuators A **333**, 113229 (2022).
[122]P. K. Das, A. D. Snider, and V. R. Bhethanabotla, "Acoustothermal heating in surface acoustic wave driven microchannel flow," Phys. Fluids **31**(10), 106106 (2019).
[123]B. H. Ha *et al.*, "Acoustothermal heating of polydimethylsiloxane microfluidic system," Sci. Rep. **5**(1), 11851 (2015).
[124]L. Meng *et al.*, "A disposable microfluidic device for controlled drug release from thermal-sensitive liposomes by high intensity focused ultrasound," Theranostics **5**(11), 1203–1213 (2015).
[125]J. Park *et al.*, "Acoustothermal tweezer for droplet sorting in a disposable microfluidic chip," Lab Chip **17**(6), 1031–1040 (2017).
[126]Y. Wang *et al.*, "A rapid and controllable acoustothermal microheater using thin film surface acoustic waves," Sens. Actuators A **318**, 112508 (2021).
[127]S. Liu *et al.*, "Investigation into the effect of acoustic radiation force and acoustic streaming on particle patterning in acoustic standing wave fields," Sensors **17**(7), 1664 (2017).
[128]A. Ozcelik *et al.*, "Acoustic tweezers for the life sciences," Nat. Methods **15**(12), 1021–1028 (2018).
[129]A. Riaud *et al.*, "Anisotropic swirling surface acoustic waves from inverse filtering for on-chip generation of acoustic vortices," Phys. Rev. Appl. **4**(3), 034004 (2015).
[130]A. Marzo and B. W. Drinkwater, "Holographic acoustic tweezers," Proc. Natl. Acad. Sci. U.S.A. **116**(1), 84–89 (2019).
[131]L. Cox *et al.*, "Acoustic hologram enhanced phased arrays for ultrasonic particle manipulation," Phys. Rev. Appl. **12**(6), 064055 (2019).
[132]A.-G. Niculescu *et al.*, "Fabrication and applications of microfluidic devices: A review," Int. J. Mol. Sci. **22**(4), 2011 (2021).
[133]S. S. Guo *et al.*, "Ultrasonic particle trapping in microfluidic devices using soft lithography," Appl. Phys. Lett. **92**(21), 213901 (2008).
[134]L. Ren *et al.*, "Standing surface acoustic wave (SSAW)-based fluorescence-activated cell sorter," Small **14**(40), 1801996 (2018).
[135]R. Amin *et al.*, "3D-printed microfluidic devices," Biofabrication **8**(2), 022001 (2016).